Neural Computing and Applications (2021) 33:12445–12475
https://doi.org/10.1007/s00521-021-05877-z

ORIGINAL ARTICLE

Multi-objective optimization of steel AISI 1040 dry turning using genetic algorithm

Djordje Vukelic[1] · Katica Simunovic[2] · Zeljko Kanovic[1] · Tomislav Saric[2] · Branko Tadic[3] · Goran Simunovic[2]

Received: 13 November 2020 / Accepted: 22 February 2021 / Published online: 7 April 2021
© The Author(s), under exclusive licence to Springer-Verlag London Ltd., part of Springer Nature 2021

Abstract
This study investigated the AISI 1040 steel turning in dry environment with four cutting inserts of different corner radii coated by CVD method. Experimental investigations were performed for different levels of cutting speeds, feeds and depths of cut using a randomized full factorial design. Quality characteristics of the workpiece machined surface were measured (arithmetical mean roughness) as well as the cutting inserts tool life characteristics (average width of flank wear). Machining times and chip volume were calculated, and based on this, chip quantity in time (material removal rate). The response surface approach and analysis of variance were used to determine the effects of input process parameters on the response variables. Based on the derived regression models, multi-objective optimization of output process parameters was performed using genetic algorithm. The objective function was simultaneous minimization of flank wear, minimization of surface roughness and maximization of material removal rate. The parameters of the genetic algorithm (crossover ratio, crossover fraction, mutation rate, Pareto front population fraction) were varied to obtain the optimal values of the objective function. Additionally, a sensitivity analysis was performed, which showed that the selected values of genetic algorithm parameters gave the best (minimum) value of objective function. Instead of the usual approach of obtaining only one combination of optimal parameters as a final solution, the basic idea was to obtain multiple combinations of optimal input process parameters depending on the importance of each output process parameter, i.e. requirements of production. Accordingly, the results of multi-objective optimization showed that there are a large number of Pareto optimal solutions. To validate the optimal input and output process values, confirmation experiments were conducted for selected trials of Pareto optimal results obtained from multi-objective optimization. A mean error percentage of 1.478% and 1.146% for flank wear and arithmetical mean roughness, respectively, proves that the predicted optimum values are confirmed by experimental results.

Keywords Turning · Arithmetical mean roughness · Flank wear · Material removal rate · AISI 1040 steel · Multi-objective optimization

1 Introduction

Up-to-date production is faced with numerous requirements such as to reduce costs, minimize time, reduce power, reduce energy consumption, maximize flexibility, increase productivity, increase quality of products and minimize negative effect on environment. All of these requirements need to be addressed in the optimal way. This is a long, often iterative process with an uncertain ending, in particular if stochastics and a great number of mutually conflicting and contradictory requirements are taken into consideration. On the other hand, a great number of

✉ Goran Simunovic
gsimunovic@unisb.hr

[1] Faculty of Technical Sciences, University of Novi Sad, Trg Dositeja Obradovica 6, 21000 Novi Sad, Serbia

[2] Mechanical Engineering Faculty in Slavonski Brod, University of Slavonski Brod, Trg Ivane Brlic Mazuranic 2, 35000 Slavonski Brod, Croatia

[3] Faculty of Engineering, University of Kragujevac, Sestre Janjic 6, 34000 Kragujevac, Serbia

experiments are necessary for a complete study of the process, which considerably increases the costs. Therefore, a balance between the number of experiments and the necessary pieces of information has to be made in order to minimize the required resources, costs and time. This is why scientific researches lay great stress on modelling, prediction and optimization of all requirements facing contemporary production. In this way, costs and time are reduced and productivity is increased. To solve the mentioned problems, various optimization techniques and methods are applied [1–4]. On the other hand, it is necessary to perform full discretization of the process in order to analyse the full region of feasible solutions and to obtain the region of optimal solutions for the given constraints. In this way, it is possible to obtain a greater number of optimal solutions of the input process parameters depending on the required output process parameters, i.e. requirements of production.

Numerous factors affect efficiency of output process parameters of machining. Their realization requires adequate technological equipment, processes, machining parameters, etc. Various machining operations are applied in mechanical engineering industry. One of the most frequently used machining operations is turning. It is mostly applied in machining cylindrical workpieces at all series levels. Using this operation, workpieces can be machined roughly, as semi-finished or finished to final measure. Workpieces from different materials can be machined by turning. Steels are a group of materials that are most often used in manufacturing engineering products. Their groups and number are various. Carbon steels belong to a special group of steels whose demand has lately been in constant increase. Significant is the application of AISI 1040 steel in different industrial sectors. This steel is used in couplings and crankshafts, as well as in production of different kinds of bolts, rods, springs, studs, etc.

Turning of workpieces made of AISI 1040 carbon steel has been researched from different perspectives and on various bases through numerous theoretical, simulation and experimental studies. Tuffy et al. [5] evaluated the influence of TiN coating thickness on the performance of turning inserts made of WC. Gunay et al. [6] evaluated the effect of rake angle on the cutting forces during turning. Yaldiz et al. [7] presented a fuzzy rule-based model for estimating the cutting forces depending on the cutting speed, feed and depth of cut. Saglam et al. [8] investigated the influence of machining parameters, rake angle and approach angle on cutting force component and temperature generated on the turning insert. Salgado and Alonso [9] presented a system for online tool wear monitoring applying the feed motor current and the sound signal. Asilturk and Cunkas [10] used multiple regression and artificial neural network (ANN) approach to estimate the surface roughness varying the cutting speeds, feeds and depths of cut. Neseli et al. [11] researched the influence of corner radius, approach angle and rake angle on the surface roughness by the use of response surface methodology (RSM). Topal and Cogun [12] proposed an ANN model for error estimation depending on cutting speed, depth of cut, feed, workpiece diameter and length. Cohen et al. [13] predicted cutting temperature by the use of the analytical model of thermal distribution on the workpiece surface by the use of ANN and multiple regression, Asiltur [14] optimized cutting speed, feed, depth of cut, and insert radius affecting the surface roughness using the Taguchi method and analysis of variance (ANOVA). Venkata Rao et al. [15] estimated the influence of turning parameters on workpiece vibration, surface roughness and volume of metal removed. Venkata Rao et al. [16] evaluated the influence of cutting speed, insert radius and feed on tool life analysing the surface roughness and workpiece vibration. Prasad et al. [17] demonstrated the 3D finite element analysis to predict the workpiece displacements in feed direction and corresponding tool wear. Venkata Rao et al. [18] applied ANN to estimate surface roughness and vibration of workpiece for different cutting speeds, feeds and nose radii. Yadav [19] analysed the influence of cutting speed, feed, primary and secondary depth of cut on average surface roughness. Haque et al. [20] optimized roughness characteristics under different cutting conditions using grey relational analysis. Akkus [21] researched the influence of cutting speed, feed and depth of cut on surface roughness by the use of Taguchi method. Jhodkar et al. [22, 23] described the comparative study of untreated and microwave treated carbide inserts at different spindle speeds, feeds and depths of cut.

Moreover, researches in the field of turning of steel have also considered and analysed the application of alternative cooling and lubricating techniques in machining aimed at minimizing the negative effect on environment. Conventional coolants and lubricants are replaced by other methods and techniques such as minimum quantity cooling lubrication (MQCL), minimum quantity lubrication (MQL), cryogenic cooling and lubrication and minimum quantity solid lubrication. Dhar et al. [24] researched the influence of cryogenic cooling on tool wear, dimensional deviation and surface quality. Dhar et al. [25] compared the performance of MQL to dry turning based on cutting temperature, chip reduction coefficient, cutting forces, tool wear, surface quality and dimensional deviation. Vamsi Krishna et al. [26] developed an empirical model to estimate the surface roughness and tool wear in turning performed by the use of solid lubricant. Ramana et al. [27] studied the influence of variation of nano level boric acid particle size on the cutting forces, tool temperatures and surface roughness. Vamsi Krishna et al. [28] studied the

effect of cutting speed and feed on temperature, flank wear and surface roughness varying the type of lubricants. Amrita et al. [29] evaluated the temperature, tool wear and cutting forces at different lubrication conditions. Srikiran et al. [30] investigated the application of nano-level particulate graphite powder as a solid lubricant during turning. Gupta et al. [31] investigated the effect of cryogenic cooling on tool wear, surface roughness, cutting forces and cutting temperature at various feeds and constant cutting speed and depth of cut. Padmini et al. [32] evaluated the main cutting force, temperature, surface roughness, and flank wear to estimate the performance of vegetable oil based nanofluids. Ajay Vardhaman et al. [33] evaluated the influence of lubricants on tool wear, friction coefficient, surface quality and chip morphology under dry, wet, coconut oil and MQL cutting conditions. Mia and Dhar [34] optimized the cutting speed, feed rate and workpiece hardness to determine minimal surface roughness using composite desirability function and genetic algorithm. Usha and Rao [35] investigated the effect of MQL flow rate, cutting speed, feed and depth of cut on cutting force, surface roughness and temperature. Sahinoglu and Rafighi [36] examined the influence of machining parameters and workpieces hardness on surface roughness and power consumption by the use of RSM and ANOVA. Gugulothu and Pasam [37] examined machining performance in turning at constant cutting conditions by the use of hybrid nanofluids under MQL.

Most of the previously mentioned researches dealt with the effects of machining parameters (cutting speed, feed, depth of cut) on the AISI 1040 carbon steel turning output process parameters. Some of the researches took into consideration cutting tool geometry, energy consumption, chip quantity, effects of coolants and lubricants, etc. The most frequently analysed output process parameters of turning were surface roughness of workpiece, cutting tool life, machining time, etc. The previously mentioned researches were performed as wet or dry turning, and some of the researches were based on the minimization of the coolants and lubricants' negative effect on environment by considering alternative techniques of cooling and lubricating. The alternative techniques of cooling and lubricating have a smaller negative effect on environment. However, negative effects are produced in these cases too, only to a lesser extent. Costs are also increased due to the additional equipment and the coolants and lubricants, the fact that can have a negative effect on expenses, particularly in the cases of small batch. In addition to experimental investigations, a small number of investigators reported on modelling and optimizing of machining performances by the application of statistical methods and artificial intelligence.

On the other hand, there are numerous studies in turning operations, but not for AISI 1040 carbon steel, in which single-objective and multi-objective optimization techniques were applied [38, 39]. The optimization of the turning process consists of two steps. In the first step, the turning process is modeled. The model describes the functional relationship between the input and output turning parameters. The methods that had the greatest application for the modeling of the turning process are: regression analysis (RA), artificial neural network (ANN), fuzzy logic (FL), support vector machine (SVM), etc. [40, 41]. When applying these methods, problems may arise in collecting data in an economical and efficient way, filtering outliers, extracting statistical characteristics of data, etc. If these problems are solved successfully, industrial application becomes possible. In the second step, after modeling the turning process, the processing parameters are optimized. Optimization determines the values of processing parameters that provide the optimal value of the appropriate optimality criterion. The optimality criterion is used to quantitatively describe the performance of the turning process. Various techniques such as ant colony optimization (ACO), simulated annealing (SA), particle swarm optimization (PSO), genetic algorithm (GA), artificial bee colony (ABC), etc., were used for optimization [42–47]. These techniques, due to the tolerance of imprecision, uncertainty and the possibility of approximation, have great application for solving highly nonlinear, multidimensional, and complex problems that occur in the turning process [48]. All modeling and optimization techniques, and as some of their combinations, have certain advantages but also disadvantages [49–53], and it is practically very difficult to define unambiguous and generally accepted criteria for the selection of modeling and optimization techniques, i.e. when and how to apply any of these techniques. Different techniques require setting the appropriate parameters, which vary depending on the selected method. In studies that determined the results obtained using different techniques, different results were obtained. No technique has shown absolute dominance over others. In fact, whether an adequate technique was chosen and whether good parameters of that same technique were chosen, can be proven only with additional-confirmation experiments and by comparing the obtained results with their prediction, i.e. with the calculation of the errors that occur. A review of the literature found that GA was very often used in turning process optimization, and that in most cases gave good results [54–60]. Furthermore, in all previous research, one optimal solution was always obtained, i.e. one optimal combination of input process parameters and one optimal output process parameter. This is not realistic, especially not from the point of view of industrial application. One optimal solution is possible only

for one combination of input process parameters. Output parameters and thus input parameters, as well as the manufacturing process, are a dynamic category [61]. It is often necessary, due to the adaptation of the turning process to the current manufacturing conditions, to change the values of turning parameters in a certain range, so it is very useful to provide more sets of optimal turning parameters in different value ranges [62]. Furthermore, in previous studies, the assessment of the validity of the developed methodology has been performed typically through one confirmation experiment, since there was only one optimal solution to be validated. In doing so, small errors in the confirmation experiment may be accidental. Therefore, it is necessary to perform a larger number of confirmation experiments to assess the validity of the applied method.

It seems that the study of the turning process based on experimental data in combination with the methods of optimization is the most promising for future researches. By combining these two approaches, one or several output process parameters can be optimized. The turning process performances can be evaluated and improved in this way. Besides, in the previous researches the variant multi-objective optimization of turning of AISI 1040 steel workpieces was not performed considering simultaneous optimization of surface roughness, tool wear and productivity. Optimal combinations of machining parameters and the cutting tool geometric and technologic characteristics depend on numerous factors in view of the fact that the turning process is characterized by a large number of the process dynamics variables. For different conditions of machining and different requirements of production, optimal parameters are also different.

Different from previous, the present research provides a multi-objective optimization of input process parameters, but for various impacts of output process parameters. In contrast to previous studies in which the main objective of optimization was to obtain one optimal combination of input process parameters, the basic idea of this research was to obtain a range, i.e. more potential Pareto optimal combinations. The main motivation was to generate optimal combinations of input process parameters (cutting speeds, feeds, depths of cut and corner radii) for various requirements of output process parameters (arithmetical surface roughness, average width of flank wear and material removal rate). In fact, it means that different combinations of input process parameters were obtained for the different weights or importance of surface quality (arithmetical mean roughness), tool life (average width of flank wear) and productivity (material removal rate). In addition, the novelty of the present paper is that a higher number of turning inserts have been used with different corner radii during the experimental research of AISI 1040 carbon steel.

2 Materials and methods

The research methodology is presented in Fig. 1. Input process parameters are the workpiece material, machining parameters which are defined on the specific machine tool and turning inserts which are located and clamped into a corresponding toolholder.

The research was conducted on workpieces made of carbon steel AISI 1040 whose chemical composition is: (98.6–99) % Fe, (0.60–0.90) % Mn, (0.37–0.44) % C, $\leq$ 0.05% S and $\leq$ 0.040% P. Furthermore, the mechanical, physical and thermal characteristics of carbon steel AISI 1040 are: density = 7.845 g/cm^3, hardness = 201 HB, tensile strength = 620 MPa, yield strength = 415 MPa, modulus of elasticity = 200 GPa, Poisson ratio = 0.29, thermal conductivity (at 0 °C) = 51.9 W/mK and thermal expansion co-efficient = 11.3 μm/m °C.

Considering the environment protection principles, the present research was conducted in dry environment. In dry machining conditions, special attention must be given to cutting tool selection and machining parameters optimization. The values of machining parameters as well as the geometric and technologic characteristics of cutting tool have to be selected in the way that they do not speed up the processes of the cutting tool wear.

Machining was performed with four turning inserts (designation: CNMG120404, CNMG120408, CNMG120412, CNMG120416) set into the same toolholder (designation: DCLBR3232M12). The turning inserts were selected in accordance with recommendations of the manufacturer, for the operation of longitudinal turning and the workpiece material AISI 1040 steel. Selected inserts are suitable for dry turning in all types of production. This is due to their geometry, material, coating process and specially designed chipbreaker.

The turning inserts differ in the size of corner radius (4 levels; r = 0.4–0.8–1.2–1.6 mm), the other geometric and technological parameters being identical:

- Grade: Duratomic grade TP2501-CVD coated,
- Coating: Ti(C,N) + Al_2O_3,
- Clearance angle major: 0°,
- Insert side clearance angle: 5°,
- Rake angle: − 6°,
- Inclination angle: − 6°,
- Lead angle: 95°,
- Insert included angle: 80°,
- Fixing hole diameter: 5.2 mm,
- Inscribed circle diameter: 12.70 mm,
- Theoretical cutting edge length: 12.90 mm.

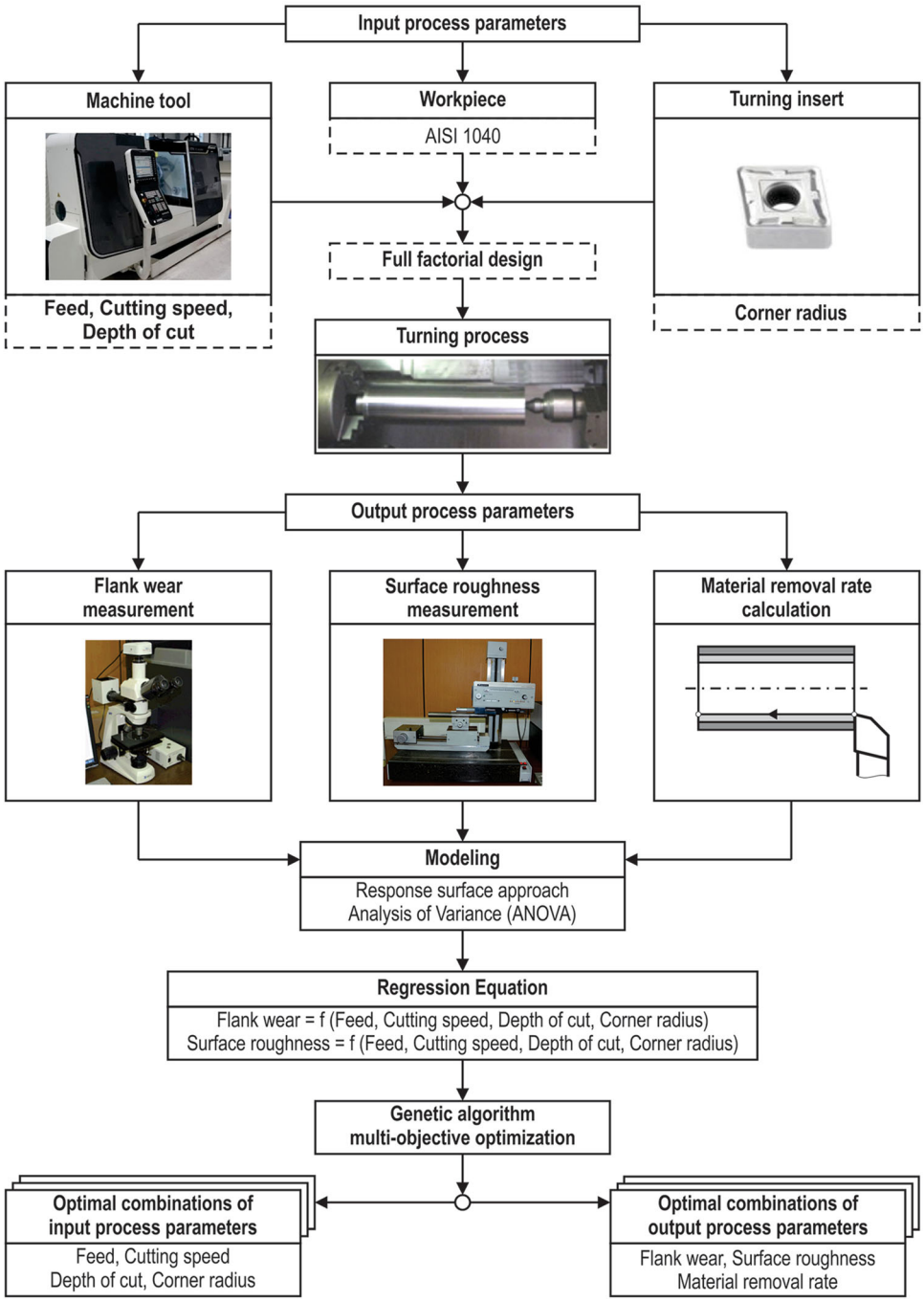

Fig. 1 Research methodology

Moreover, based on the manufacturer of the turning inserts, the following machining parameters were selected:

- 4 levels for feed, f = 0.1–0.2–0.3–0.4 (mm/rev),
- 3 levels for cutting speed, v_c = 300–350–400 (mm/min),
- 3 levels for depth of cut, a_p = 2–2.5–3 (mm).

The machine tool used for machining was CNC lathe DMG Mori Seiki CTX. Locating and clamping of workpiece was performed by means of the chuck and rotating centre. Machine tool and fixtures were selected so that the machining could be performed reliably, with high accuracy and stability of the machining process, aimed at minimizing vibrations of the workpiece and compliance of the workpiece-fixtures system. The original workpiece diameter was Ø60 mm and the length was 450 mm. Turning was carried out in 5 passes. For each experiment, a new turning insert was used.

Experimental research was conducted in accordance with randomized full factorial design, which enabled the

research of all combinations of levels of input variables. Considering the fact that 4 levels were adopted for corner radius, 4 levels for feed, 3 levels for cutting speed and 3 levels for depth of cut, total number of experiments was $4 \times 4 \times 3 \times 3 = 144$.

After the experimental researches, the turning insert flank wear and the machined surface roughness were measured. The turning insert flank wear *VB* measuring was carried out on MT8500 microscope. Surface roughness measurement (of parameter *Ra*) was conducted on measuring instrument Talysurf with probe tip radius $r_t = 2$ µm. Measurement was performed with a cut-off length of 0.8 mm and sampling length of 4 mm. Roughness was measured in 3 directions moved by 120 degrees in relation to the workpiece axis. The surface roughness *Ra* values were calculated as average values from three different directions of measuring.

Material removal rate (chip quantity in time) was calculated by equation [63]:

$$Q = \frac{V}{t}\left(\mathrm{mm}^3/\mathrm{s}\right) \tag{1}$$

where V is total chip volume, t is turning time.

Turning time for the ith pass at external longitudinal turning equals [63]:

$$t_i = \frac{60 \cdot l_i}{f_i \cdot n_i}\,(\mathrm{s}) \tag{2}$$

where l_i (mm) is turning length for the ith pass, f_i (mm/rev) is feed for the ith pass, and n_i (rev/min) is number of revolutions for the ith pass.

Number of revolutions for the ith pass equals [63]:

$$n_i = \frac{1000 \cdot v_{ci}}{\pi \cdot d_i}\,(\mathrm{rev/min}) \tag{3}$$

where v_{ci} (m/min) is cutting speed for the ith pass, d_i (mm) is diameter after the ith pass.

Diameter after the ith pass equals [63]:

$$d_i = d_k - 2 \cdot a_{pi}\,(\mathrm{mm}) \tag{4}$$

where d_k (mm) is diameter before the ith pass, a_{pi} (mm) is depth of cut for the ith pass.

Substitution of Eqs. (3) and (4) into Eq. (2) gives the turning time for the ith pass:

$$t_i = \frac{60 \cdot l_i}{f_i \cdot \frac{1000 \cdot v_{ci}}{\pi \cdot d_i}} = \frac{60 \cdot \pi \cdot l_i \cdot d_i}{f_i \cdot 1000 \cdot v_{ci}} = \frac{60 \cdot \pi \cdot l_i \cdot \left(d_k - 2 \cdot a_{pi}\right)}{f_i \cdot 1000 \cdot v_{ci}}\,(\mathrm{s}) \tag{5}$$

If machining is performed with constant cutting speed ($v_c = v_{ci}$ = const), constant feed ($f = f_i$ = const), constant depth of cut ($a_p = a_{pi}$ = const) and at constant length of cut ($l = l_i$ = const), machining time for the ith pass is:

$$t_i = \frac{60 \cdot \pi \cdot l \cdot d_i}{f \cdot 1000 \cdot v_c} = \frac{60 \cdot \pi \cdot l \cdot \left(d_k - 2 \cdot a_p\right)}{f \cdot 1000 \cdot v_c}\,(\mathrm{s}) \tag{6}$$

For the machining in n passes, total turning time is:

$$t = \sum_{i=1}^{n} t_i\,(\mathrm{s}) \tag{7}$$

where n is total number of passes.

Chip volume for the ith pass is equal to the volume before and after the ith pass:

$$V_i = \left(\left(\frac{d_k}{2}\right)^2 - \left(\frac{d_i}{2}\right)^2\right) \cdot \pi \cdot l_i\left(\mathrm{mm}^3\right) \tag{8}$$

Substitution of Eq. (4) to (8) gives:

$$V_i = \left(\left(\frac{d_k}{2}\right)^2 - \left(\frac{d_k - 2 \cdot a_{pi}}{2}\right)^2\right) \cdot \pi \cdot l_i\left(\mathrm{mm}^3\right) \tag{9}$$

For turning in n passes, total chip volume equals:

$$V = \sum_{i=1}^{n} V_i\left(\mathrm{mm}^3\right) \tag{10}$$

If several passes machining is performed with constant depth of cut ($a_p = a_{pi}$ = const) and at constant length of cut ($l = l_i$ = const) total chip volume equals:

$$V = \sum_{i=1}^{n} V_i = \left(\left(\frac{d_{\max}}{2}\right)^2 - \left(\frac{d_{\min}}{2}\right)^2\right) \cdot \pi \cdot l\left(\mathrm{mm}^3\right) \tag{11}$$

where $d_{\max}$ is original diameter, $d_{\min}$ is final diameter.

As final diameter of machining equals:

$$d_{\min} = d_{\max} - 2 \cdot a_p \cdot i\,(\mathrm{mm}) \tag{12}$$

Substitution of Eq. (12) to (11) gives total chip volume after i passes, at constant depth of cut ($a_p = a_{pi}$ = const) and constant length of cut ($l = l_i$ = const), being equal to:

$$V = \left(\left(\frac{d_{\max}}{2}\right)^2 - \left(\frac{d_{\max} - 2 \cdot a_p \cdot i}{2}\right)^2\right) \cdot \pi \cdot l\left(\mathrm{mm}^3\right) \tag{13}$$

In case the machining is carried out with constant cutting speed ($v_c = v_{ci}$ = const), constant feed ($f = f_i$ = const), constant depth of cut ($a_p = a_{pi}$ = const) and at constant length of cut ($l = l_i$ = const), chip quantity in time (material removal rate) equals:

$$Q = \frac{V}{t} = \frac{\left(\left(\frac{d_{\max}}{2}\right)^2 - \left(\frac{d_{\max} - 2 \cdot a_p \cdot i}{2}\right)^2\right) \cdot \pi \cdot l}{\sum_{i=1}^{n} \frac{60 \cdot \pi \cdot l \cdot d_i}{f \cdot 1000 \cdot v_c}}\left(\mathrm{mm}^3/\mathrm{s}\right) \tag{14}$$

Following the performed experimental investigations, statistical processing, i.e. regression modelling, was conducted for obtained results. The regression modelling was conducted for different levels of four factors, i.e. four input parameters—corner radius (r), cutting speed (v_c), feed

(f) and depth of cut (a_p). After obtaining regression equations, transformation and reduction were performed in order to obtain models with a high coefficient of determination to predict the measured responses (output process parameters)—flank wear of turning insert (VB) and surface roughness (Ra). Analysis of variance (ANOVA) was performed, as well as diagnostics and adequacy checking of regression models.

Multi-objective optimization is suitable for solving complex optimization problems whose individual objective functions are conflicting, i.e. one is opposed to the other. In this paper, GA is applied to multi-objective optimization. The main idea is to determine the optimal values of input process parameters (cutting speeds, feeds, depths of cut and corner radii) in order to minimize the flank wear (VB) and the surface roughness (Ra) and at the same time to maximize the material removal rate (Q). These quantities are expressed using regression model, described in the next chapter.

To conduct the multi-objective optimization, some modification of standard GA must be made. In this research, a version of elitist genetic algorithm [64] is used, which favours individuals with better fitness value. Also, some boundary constraints to input parameters, described in detail in the next chapter, must be obeyed during the optimization.

The input process parameters (cutting speeds, feeds, depths of cut) are real numbers in different, given ranges, and corner radii have discrete values, as mentioned before, which represent boundary-type constraints (the solution must be within these given constraints). Total number of parameters, i.e. variables, is four. Therefore, GA individuals are defined as vectors of four values representing these parameters.

The algorithm starts by creating the initial population, consisting of known number of individuals, defined as population size. The individuals are created randomly, using uniform distribution, and considering the feasible space defined by boundary constraints. The fitness function is then evaluated for each individual. According to the fitness value, all individuals are ranked in the following way:

- All undominated individuals [64] have the rank 1.
- Rank 2 individuals are those dominated only by rank 1 individuals. In general, rank k is given to individuals dominated by individuals of rank $k - 1$ and lower.
- Having in mind that during the optimization process some infeasible individuals can occur, their rank value is always worse than of any feasible individual. Among the infeasible part of population, the rank is sorted by the infeasibility measure (individuals with less feasibility discrepancy have lower rank).

After the ranking procedure is conducted, the next phase of the algorithm is selection. The individuals are selected using binary tournament selection function. Two pairs of individuals are chosen randomly, and the ranks of individuals in each pair are compared. The individual with lower rank is selected. If the individuals have the same rank, the one with higher distance measure is selected. Distance measure shows how far the individual is from the other individuals of the same rank [64]. In this way, the population diversity is kept during the optimization process. The "wining" individuals from both pairs are chosen as parents.

The next step is the crossover phase. As the variables are dominantly real numbers, heuristic crossover has been used, meaning that the new individual (child) is created on the line containing both parents, in the vicinity of the better ranked parent. The parameter named crossover ratio determines how far from the better parent will a child be positioned. This parameter is usually taken in the range [0.8, 1.6]. The value 1.2, for example, means that the child is positioned away from the better parent at the distance of 20% of total distance between parents, in the direction opposite to the worse parent.

After the crossover, the mutation operator will be applied. Mutation means that some fractions of individuals will be changed. The probability of mutation for each fraction of individual (i.e. the variable) is determined by parameter named mutation rate, usually taken in the range [0.005, 0.02]. The fractions chosen for mutation are then replaced by random number selected uniformly from the range for that variable.

Final step consists of creation of new generation of individuals. The new generation consists of two parts. First part represents elite individuals, i.e. a part of the Pareto set of the current generation, determined by the parameter named Pareto front population fraction. The value of this parameter is usually in the range [0.2, 0.5], meaning that 20–50% of Pareto set will be kept for the next generation, as elite individuals. The second part of new generation is created by crossover and mutation. The number of individuals created by crossover is determined by parameter named crossover fraction, which is usually in the range [0.7, 0.9], meaning that 70–90% of this part is created by crossover, while the rest of the individuals are the result of mutation.

The described procedure is repeated for a given number of iterations. After the final iteration is completed, the undominated individuals, creating the Pareto front for the considered multi-objective optimization problem, are taken as a solution.

After the multi-objective optimization, optimal combinations of output process parameters (VB_{opt}, Ra_{opt}, Q_{opt}) are obtained with the corresponding optimal combinations

of input process parameters (f_{opt}, v_{copt}, a_{popt}, r_{opt}). After generating optimal values of input and output process parameters confirmation experiments were conducted to validate the use of genetic algorithm for multi-objective optimization. Finally, the obtained results were analysed and discussed.

3 Results and discussion

3.1 Experimental research

Results of measuring and calculating output process parameters for different combinations of input process parameters are displayed in Table 1.

Obtained results point to the significant dispersion of results. Appropriate selection and various combinations of cutting speed, feed, depth of cut and corner radius can result in different values of surface roughness, flank wear and material removal rate. In other words, appropriate selection i.e. appropriate combination of input process parameters, can significantly affect output process parameters. In the conducted experimental researches, depending on the input process parameters, flank wear appears in the wide range from 0.147 to 0.293 mm. This means that lower but also higher flank wear can be obtained by the appropriate choice of the input process parameters. The lowest flank wear ($VB = VB_{min} = 0.147$ mm) is achieved at machining with the lowest values of machining parameters ($v_c = v_{cmin} = 300$ m/min, $f = f_{min} = 0.1$ mm/rev, $a_p = a_{pmin} = 2$ mm) and the highest corner radius ($r = r_{max} = 1.6$ mm), but then the chip quantity in time is also the lowest ($Q = Q_{min} = 1041.67$ mm^3/s). The highest flank wear ($VB = VB_{max} = 0.293$ mm) is obtained at machining with the highest values of machining parameters ($v_c = v_{cmax} = 400$ m/min, $f = f_{max} = 0.4$ mm/rev, $a_p = a_{pmax} = 3$ mm) and the lowest corner radius ($r = r_{min} = 0.4$ mm), but then the chip quantity in time is also the highest ($Q = Q_{max} = 8571.43$ mm^3/s).

Results of experimental research reveal that smaller roughness of machined surface and smaller flank wear are obtained at higher corner radii of turning insert, smaller feeds, smaller cutting speeds and smaller depths of cut. Different from this, shorter turning time and higher chip quantity are obtained at higher cutting speeds, higher feeds and higher depths of cut. It actually means that better quality of machined surface and longer tool life are obtained if corner radius is at maximal level and machining parameters at minimal level. Different from this, the highest material removal rate is reached if machining parameters are at maximal level. It is evident that there are conflicting requirements if output process parameters are considered separately, i.e. independently ones from the others (Table 2).

3.2 Regression modelling

Statistical processing of measured data for *VB* and *Ra* is carried out by Design Expert software. Significant quadratic, transformed and reduced regression models are obtained (non-significant terms with the probability of type I error, p value, greater than 0.05 are removed).

Final equations in terms of actual factors are shown in Tables 3 (for *VB*) and 4 (for *Ra*) for each level of turning insert type (corner radius r) as a categorical factor.

Tables 5 and 6 present the analysis of variance (ANOVA) for the regression model for *VB* and for *Ra*. These tables also present the coefficients of determination: R^2, R^2 adjusted and R^2 for prediction, as well as the other ANOVA output (adequate precision, standard deviation, mean, coefficient of variation, predicted residual sum of squares).

From Tables 5 and 6, it is visible that the regression models for *VB* and *Ra* are statistically significant because the probabilities for the F variable, i.e. p values are smaller than 0.05 (probability of type I error, i.e. significance level). It means that the null hypothesis should be rejected and alternative one accepted (at least one of the regression variables significantly contributes to the model, i.e. has a regression coefficient different from zero).

Normal probability plots of the internally studentized residuals to check for normality are shown in Fig. 2a (for *VB*) and b (for *Ra*).

Graphical presentations of internally studentized residuals versus predicted values (obtained by regression models) to check for constant error are given in Fig. 3a (for *VB*) and b (for *Ra*). It is visible from Figs. 2a and 3a that out of 144 internally studentized residuals, there is deviation of only 3 data for *VB* (− 5.145, 4.686 and 4.682 for runs 40, 90 and 120, Table 1), while in Figs. 2b and 3b the question is about the deviation of only 2 data for *Ra* (− 3.453 and − 3.327 for runs 15 and 105, Table 1).

Externally studentized residuals to look for outliers, i.e. influential values (Fig. 4a, b), show that for runs 40, 90 and 120 (Table 1) for *VB* there are deviations out of limits (Fig. 4a), while it is not the case for *Ra* (Fig. 4b) for runs 15 and 105, Table 1. However, for runs 90 and 120 (Table 1) for *VB*, for measures DFFITS (Difference in fits) and Cook's distance there is no deviation in relation to other runs (they are 1.8204, 1.8183 and 0.23197, 0.23152, respectively). These measures do not deviate from other runs even for runs 15 and 105, Table 1 for *Ra* (they are − 1.6593, − 1.4289 and 0.15728, 0.11748, respectively). Out of 5 analysed runs (3 for *VB* and 2 for *Ra*), only for run 40, Table 1, for *VB*, there is measure DFFITS which has a

Table 1 Results of measuring and calculating

Run	Input process parameters				Output process parameters				
	r (mm)	f (mm/rev)	v_c (m/min)	a_p (mm)	VB (mm)	Ra (μm)	t (s)	V (mm^3)	Q (mm^3/s)
1	1.2	0.3	300	3	0.180	4.211	197.82	953,775.00	4821.43
2	0.4	0.2	300	3	0.210	6.790	296.73	953,775.00	3214.29
3	1.2	0.3	350	2.5	0.199	4.061	181.67	838,968.75	4618.06
4	0.4	0.3	300	3	0.223	15.126	197.82	953,775.00	4821.43
5	0.8	0.1	400	2.5	0.219	0.689	476.89	838,968.75	1759.26
6	1.2	0.1	300	2.5	0.156	0.444	635.85	838,968.75	1319.44
7	0.8	0.4	300	3	0.209	11.208	148.37	953,775.00	6428.57
8	1.2	0.2	350	2	0.187	1.705	290.67	706,500.00	2430.56
9	0.4	0.4	400	2	0.284	22.884	127.17	706,500.00	5555.56
10	1.6	0.3	400	3	0.214	3.265	148.37	953,775.00	6428.57
11	0.8	0.2	400	3	0.234	2.980	222.55	953,775.00	4285.71
12	1.6	0.2	350	2.5	0.181	1.356	272.51	838,968.75	3078.70
13	1.2	0.4	350	3	0.213	7.612	127.17	953,775.00	7500.00
14	0.8	0.1	400	2	0.217	0.655	508.68	706,500.00	1388.89
15	0.4	0.1	300	3	0.197	1.685	593.46	953,775.00	1607.14
16	0.8	0.2	350	3	0.211	2.859	254.34	953,775.00	3750.00
17	0.8	0.2	350	2.5	0.207	2.709	272.51	838,968.75	3078.70
18	1.2	0.4	300	2	0.186	6.661	169.56	706,500.00	4166.67
19	1.2	0.2	350	2.5	0.189	1.805	272.51	838,968.75	3078.70
20	0.4	0.1	400	2.5	0.248	1.581	476.89	838,968.75	1759.26
21	1.2	0.4	400	2	0.229	6.937	127.17	706,500.00	5555.56
22	0.4	0.4	350	2.5	0.261	24.843	136.25	838,968.75	6157.41
23	1.2	0.1	350	3	0.182	0.478	508.68	953,775.00	1875.00
24	0.8	0.4	300	2	0.203	10.005	169.56	706,500.00	4166.67
25	1.6	0.3	400	2.5	0.211	3.095	158.96	838,968.75	5277.78
26	1.6	0.3	350	3	0.193	3.209	169.56	953,775.00	5625.00
27	1.2	0.4	350	2.5	0.212	7.211	136.25	838,968.75	6157.41
28	1.6	0.3	350	2	0.188	2.868	193.78	706,500.00	3645.83
29	1.2	0.3	300	2.5	0.177	3.978	211.95	838,968.75	3958.33
30	0.4	0.2	400	2.5	0.261	6.325	238.44	838,968.75	3518.52
31	0.4	0.4	400	2.5	0.287	25.309	119.22	838,968.75	7037.04
32	1.6	0.4	300	3	0.182	5.611	148.37	953,775.00	6428.57
33	1.2	0.3	400	3	0.224	4.361	148.37	953,775.00	6428.57
34	1.2	0.2	400	2.5	0.211	1.838	238.44	838,968.75	3518.52
35	1.6	0.4	350	2.5	0.202	5.411	136.25	838,968.75	6157.41
36	1.6	0.1	300	3	0.152	0.361	593.46	953,775.00	1607.14
37	0.4	0.1	300	2	0.191	1.373	678.24	706,500.00	1041.67
38	1.2	0.1	400	2.5	0.201	0.458	476.89	838,968.75	1759.26
39	1.2	0.3	350	3	0.202	4.279	169.56	953,775.00	5625.00
40	1.6	0.4	400	3	0.221	5.815	111.27	953,775.00	8571.43
41	1.6	0.2	400	2.5	0.201	1.378	238.44	838,968.75	3518.52
42	0.4	0.2	350	3	0.237	6.849	254.34	953,775.00	3750.00
43	1.2	0.2	300	3	0.170	1.866	296.73	953,775.00	3214.29
44	0.8	0.1	350	2	0.193	0.636	581.35	706,500.00	1215.28
45	0.8	0.3	300	2	0.192	5.623	226.08	706,500.00	3125.00
46	0.8	0.3	300	2.5	0.194	5.964	211.95	838,968.75	3958.33
47	0.4	0.2	350	2.5	0.234	6.214	272.51	838,968.75	3078.70

Table 1 (continued)

Run	Input process parameters				Output process parameters				
	r (mm)	f (mm/rev)	v_c (m/min)	a_p (mm)	VB (mm)	Ra (μm)	t (s)	V (mm^3)	Q (mm^3/s)
48	1.2	0.4	350	2	0.208	6.806	145.34	706,500.00	4861.11
49	0.4	0.3	350	2	0.244	12.628	193.78	706,500.00	3645.83
50	1.6	0.1	300	2.5	0.149	0.333	635.85	838,968.75	1319.44
51	1.6	0.1	400	2	0.189	0.325	508.68	706,500.00	1388.89
52	0.4	0.4	300	2.5	0.232	24.384	158.96	838,968.75	5277.78
53	1.2	0.3	350	2	0.197	3.825	193.78	706,500.00	3645.83
54	1.2	0.4	300	2.5	0.187	7.067	158.96	838,968.75	5277.78
55	1.2	0.1	400	3	0.203	0.488	445.10	953,775.00	2142.86
56	0.8	0.4	350	2	0.228	10.205	145.34	706,500.00	4861.11
57	0.8	0.3	350	2	0.216	5.735	193.78	706,500.00	3645.83
58	0.8	0.3	350	2.5	0.218	6.079	181.67	838,968.75	4618.06
59	0.8	0.3	400	2.5	0.242	6.184	158.96	838,968.75	5277.78
60	0.8	0.4	400	2.5	0.254	11.011	119.22	838,968.75	7037.04
61	1.2	0.2	300	2.5	0.166	1.769	317.93	838,968.75	2638.89
62	1.6	0.1	300	2	0.147	0.313	678.24	706,500.00	1041.67
63	1.6	0.3	300	3	0.172	3.159	197.82	953,775.00	4821.43
64	1.2	0.1	400	2	0.198	0.437	508.68	706,500.00	1388.89
65	0.4	0.2	300	2.5	0.206	6.095	317.93	838,968.75	2638.89
66	0.8	0.1	300	3	0.174	0.711	593.46	953,775.00	1607.14
67	0.8	0.4	350	3	0.233	11.411	127.17	953,775.00	7500.00
68	0.8	0.2	300	3	0.186	2.807	296.73	953,775.00	3214.29
69	1.6	0.1	400	3	0.194	0.368	445.10	953,775.00	2142.86
70	1.6	0.4	400	2.5	0.221	5.507	119.22	838,968.75	7037.04
71	1.2	0.2	350	3	0.192	1.909	254.34	953,775.00	3750.00
72	0.8	0.3	300	3	0.197	6.307	197.82	953,775.00	4821.43
73	0.4	0.1	350	2.5	0.221	1.554	545.01	838,968.75	1539.35
74	0.4	0.4	300	2	0.230	22.005	169.56	706,500.00	4166.67
75	0.4	0.4	350	2	0.257	22.437	145.34	706,500.00	4861.11
76	1.6	0.4	350	2	0.198	5.107	145.34	706,500.00	4861.11
77	0.4	0.1	350	2	0.218	1.402	581.35	706,500.00	1215.28
78	1.2	0.3	300	2	0.175	3.752	226.08	706,500.00	3125.00
79	0.4	0.4	350	3	0.263	27.368	127.17	953,775.00	7500.00
80	1.2	0.1	350	2.5	0.178	0.456	545.01	838,968.75	1539.35
81	0.8	0.4	350	2.5	0.231	10.811	136.25	838,968.75	6157.41
82	0.4	0.1	300	2.5	0.193	1.523	635.85	838,968.75	1319.44
83	0.4	0.3	350	3	0.251	15.396	169.56	953,775.00	5625.00
84	1.2	0.2	400	2	0.208	1.736	254.34	706,500.00	2777.78
85	1.6	0.2	300	3	0.162	1.409	296.73	953,775.00	3214.29
86	1.6	0.2	400	3	0.204	1.461	222.55	953,775.00	4285.71
87	0.4	0.3	400	2.5	0.274	14.237	158.96	838,968.75	5277.78
88	1.2	0.1	300	2	0.154	0.419	678.24	706,500.00	1041.67
89	1.2	0.4	400	3	0.235	7.739	111.27	953,775.00	8571.43
90	0.4	0.1	400	3	0.256	1.749	445.10	953,775.00	2142.86
91	1.2	0.3	400	2.5	0.221	4.123	158.96	838,968.75	5277.78
92	0.8	0.2	300	2.5	0.182	2.650	317.93	838,968.75	2638.89
93	0.4	0.4	300	3	0.236	26.886	148.37	953,775.00	6428.57
94	0.4	0.3	400	3	0.278	15.702	148.37	953,775.00	6428.57

Table 1 (continued)

Run	Input process parameters				Output process parameters				
	r (mm)	f (mm/rev)	v_c (m/min)	a_p (mm)	VB (mm)	Ra (μm)	t (s)	V (mm^3)	Q (mm^3/s)
95	1.6	0.1	350	2	0.168	0.318	581.35	706,500.00	1215.28
96	1.6	0.2	400	2	0.199	1.304	254.34	706,500.00	2777.78
97	0.4	0.4	400	3	0.293	27.851	111.27	953,775.00	8571.43
98	1.2	0.1	300	3	0.159	0.471	593.46	953,775.00	1607.14
99	1.6	0.1	400	2.5	0.191	0.343	476.89	838,968.75	1759.26
100	0.4	0.3	300	2	0.217	12.371	226.08	706,500.00	3125.00
101	0.8	0.3	400	2	0.240	5.854	169.56	706,500.00	4166.67
102	1.2	0.3	400	2	0.219	3.905	169.56	706,500.00	4166.67
103	1.6	0.2	300	2.5	0.159	1.328	317.93	838,968.75	2638.89
104	1.2	0.4	400	2.5	0.232	7.334	119.22	838,968.75	7037.04
105	0.4	0.1	350	3	0.225	1.711	508.68	953,775.00	1875.00
106	0.8	0.2	400	2.5	0.231	2.759	238.44	838,968.75	3518.52
107	0.4	0.2	300	2	0.204	5.503	339.12	706,500.00	2083.33
108	0.4	0.2	400	3	0.265	6.990	222.55	953,775.00	4285.71
109	1.2	0.2	400	3	0.214	1.938	222.55	953,775.00	4285.71
110	1.6	0.3	400	2	0.209	2.925	169.56	706,500.00	4166.67
111	1.2	0.1	350	2	0.176	0.424	581.35	706,500.00	1215.28
112	0.8	0.1	300	2.5	0.171	0.664	635.85	838,968.75	1319.44
113	0.4	0.1	400	2	0.245	1.434	508.68	706,500.00	1388.89
114	0.8	0.1	400	3	0.223	0.729	445.10	953,775.00	2142.86
115	1.6	0.4	300	2	0.177	5.009	169.56	706,500.00	4166.67
116	0.4	0.3	350	2.5	0.247	13.976	181.67	838,968.75	4618.06
117	0.8	0.3	400	3	0.246	6.533	148.37	953,775.00	6428.57
118	0.8	0.2	300	2	0.180	2.509	339.12	706,500.00	2083.33
119	0.4	0.2	400	2	0.258	5.725	254.34	706,500.00	2777.78
120	0.8	0.4	400	3	0.261	11.621	111.27	953,775.00	8571.43
121	0.8	0.4	300	2.5	0.205	10.609	158.96	838,968.75	5277.78
122	1.6	0.2	350	2	0.178	1.275	290.67	706,500.00	2430.56
123	0.8	0.1	300	2	0.169	0.624	678.24	706,500.00	1041.67
124	1.6	0.4	350	3	0.203	5.714	127.17	953,775.00	7500.00
125	1.6	0.3	350	2.5	0.191	3.013	181.67	838,968.75	4618.06
126	1.2	0.2	300	2	0.165	1.669	339.12	706,500.00	2083.33
127	0.8	0.1	350	2.5	0.195	0.675	545.01	838,968.75	1539.35
128	1.6	0.3	300	2	0.167	2.812	226.08	706,500.00	3125.00
129	0.8	0.1	350	3	0.198	0.714	508.68	953,775.00	1875.00
130	0.8	0.2	350	2	0.204	2.554	290.67	706,500.00	2430.56
131	0.4	0.3	300	2.5	0.219	13.719	211.95	838,968.75	3958.33
132	0.4	0.3	400	2	0.271	12.872	169.56	706,500.00	4166.67
133	0.4	0.2	350	2	0.231	5.612	290.67	706,500.00	2430.56
134	1.6	0.4	400	2	0.219	5.207	127.17	706,500.00	5555.56
135	1.6	0.3	300	2.5	0.169	2.983	211.95	838,968.75	3958.33
136	1.6	0.2	300	2	0.157	1.253	339.12	706,500.00	2083.33
137	1.6	0.1	350	3	0.173	0.359	508.68	953,775.00	1875.00
138	1.2	0.4	300	3	0.191	7.469	148.37	953,775.00	6428.57
139	1.6	0.2	350	3	0.183	1.429	254.34	953,775.00	3750.00
140	0.8	0.4	400	2	0.251	10.407	127.17	706,500.00	5555.56
141	1.6	0.4	300	2.5	0.179	5.311	158.96	838,968.75	5277.78

Table 1 (continued)

Run	Input process parameters				Output process parameters				
	r (mm)	f (mm/rev)	v_c (m/min)	a_p (mm)	VB (mm)	Ra (μm)	t (s)	V (mm^3)	Q (mm^3/s)
142	1.6	0.1	350	2.5	0.171	0.334	545.01	838,968.75	1539.35
143	0.8	0.2	400	2	0.228	2.603	254.34	706,500.00	2777.78
144	0.8	0.3	350	3	0.222	6.414	169.56	953,775.00	5625.00
Minimum					0.147	0.313	111.27	706,500.00	1041.67
Maximum					0.293	27.851	678.24	953,775.00	8571.43
Mean					0.208	5.663	287.80	833,081.25	3858.03
Standard deviation					0.032	6.266	166.95	101,388.06	1948.78
Ratio					1.993	88.981	6.095	1.350	8.229

Table 2 Optimal values of input process parameters if output process parameters are considered independently one from the other

Turning parameters	Minimum VB VB = 0.147 (mm)	Minimum Ra Ra = 0.313 (μm)	Maximum Q Q = 8571.43 (mm^3/s)
v_c (m/min)	300	300	400
f (mm/rev)	0.1	0.1	0.4
a_p (mm)	2	2	3
r (mm)	1.6	1.6	–

value different from other runs (it is − 2.04), however with a good indicator of Cook's distance (it is 0.2796).

After the conducted diagnostics of regression models, it can be concluded that the models can be applied as inputs for multi-objective optimization as, in addition to the above-mentioned analysis connected with outliers and influential values (Figs. 2, 3, 4), the other indicators are also very good (high and equivalent values of Adj R-Squared and Pred R-Squared, small MSE, that is, $St.\ Dev.$, small values of indicator $PRESS$ and high values of indicator Adeq Precision), which can be seen from Tables 5 and 6. Furthermore, the correlation between measured and predicted regression values for VB and Ra is given in Fig. 5. Evaluation of obtained results was performed based on the following errors and coefficient [64]:

$$MAE_x = \frac{1}{n}\sum_{i=1}^{n}\left|x_{ipv} - x_{imv}\right| \quad i = 1, 2, \ldots, 144 \quad x = VB, Ra \tag{15}$$

$$RMSE_x = \sqrt{\frac{\sum_{i=1}^{n}\left(x_{ipv} - x_{imv}\right)^2}{n}} \quad i = 1, 2, \ldots, 144 \quad x = VB, Ra \tag{16}$$

$$MRE_x = \frac{1}{n}\sum_{i=1}^{n}\left|\frac{x_{ipv} - x_{imv}}{x_{imv}}\right| \quad i = 1, 2, \ldots, 144 \quad x = VB, Ra \tag{17}$$

$$R_x = \sqrt{\sum_{i=1}^{n} x_{imv}^2 - \frac{\sum_{i=1}^{n}\left(x_{ipv} - x_{imv}\right)^2}{\sum_{i=1}^{n} x_{imv}^2}} \quad i = 1, 2, \ldots, 144 \quad x = VB, Ra \tag{18}$$

where MAE—mean absolute error, $RMSE$—root mean square error, MRE—mean relative error, R—coefficient of correlation, x_{ipv}—predicted value, x_{imv}—measured value.

The statistical measures—mean absolute error (MAE), root mean square error ($RMSE$), mean relative error (MRE) and coefficient of correlation (R) given in Table 7 prove that there is a very strong correlation between measured and predicted values obtained by the regression models. Finally, the calculated p values for the correlation are much smaller than 0.05 which means that the correlation is statistically significant (i.e. alternative hypothesis at significance level of 0.05 should be accepted).

The results of regression analysis show that smaller flank wear, i.e. higher turning insert life is obtained at smaller depths of cut, smaller feeds, smaller cutting speeds and higher corner radii of turning inserts (Fig. 6). In this process, the highest influence on flank wear is exerted by the corner radius of turning insert (correlation coefficient, r = − 0.655), somewhat smaller is the influence of cutting speed (r = 0.614), even smaller is the influence of feed (r = 0.400), and the smallest is the influence of depth of cut (r = 0.075).

Table 3 Regression equations for flank wear *VB* for each corner radius *r*

Corner radius *r* (mm)	Regression equation
0.4	$\ln VB = -2.902316273 - 0.009204749 \cdot a_p + 1.095838685 \cdot f + 0.00484147 \cdot v_c - 0.017319213 \cdot a_p \cdot f - 0.00128037 \cdot f \cdot v_c + 0.008257836 \cdot a_p^2 - 0.114209488 \cdot f^2 - 3.18162 \cdot 10^{-6} \cdot v_c^2$
0.8	$\ln VB = -3.025348666 - 0.009204749 \cdot a_p + 1.095838685 \cdot f + 0.00484147 \cdot v_c - 0.017319213 \cdot a_p \cdot f - 0.00128037 \cdot f \cdot v_c + 0.008257836 \cdot a_p^2 - 0.114209488 \cdot f^2 - 3.18162 \cdot 10^{-6} \cdot v_c^2$
1.2	$\ln VB = -3.11644376 - 0.009204749 \cdot a_p + 1.095838685 \cdot f + 0.00484147 \cdot v_c - 0.017319213 \cdot a_p \cdot f - 0.00128037 \cdot f \cdot v_c + 0.008257836 \cdot a_p^2 - 0.114209488 \cdot f^2 - 3.18162 \cdot 10^{-6} \cdot v_c^2$
1.6	$\ln VB = -3.16345538 - 0.009204749 \cdot a_p + 1.095838685 \cdot f + 0.00484147 \cdot v_c - 0.017319213 \cdot a_p \cdot f - 0.00128037 \cdot f \cdot v_c + 0.008257836 \cdot a_p^2 - 0.114209488 \cdot f^2 - 3.18162 \cdot 10^{-6} \cdot v_c^2$

Table 4 Regression equations for surface roughness *Ra* for each corner radius *r*

Corner radius *r* (mm)	Regression equation
0.4	$Ra^{0.37} = 0.09778824 + 0.102695042 \cdot a_p + 7.562630695 \cdot f + 5.2741 \cdot 10^{-5} \cdot v_c + 0.260760914 \cdot a_p \cdot f + 0.000713465 \cdot f \cdot v_c - 2.924702941 \cdot f^2$
0.8	$Ra^{0.37} = 0.204364402 + 0.00547981 \cdot a_p + 5.703020293 \cdot f + 5.2741 \cdot 10^{-5} \cdot v_c + 0.260760914 \cdot a_p \cdot f + 0.000713465 \cdot f \cdot v_c - 2.924702941 \cdot f^2$
1.2	$Ra^{0.37} = 0.178414942 - 0.005411175 \cdot a_p + 4.98566363 \cdot f + 5.2741 \cdot 10^{-5} \cdot v_c + 0.260760914 \cdot a_p \cdot f + 0.000713465 \cdot f \cdot v_c - 2.924702941 \cdot f^2$
1.6	$Ra^{0.37} = 0.156616488 - 0.010167075 \cdot a_p + 4.540891052 \cdot f + 5.2741 \cdot 10^{-5} \cdot v_c + 0.260760914 \cdot a_p \cdot f + 0.000713465 \cdot f \cdot v_c - 2.924702941 \cdot f^2$

In this research, only fine tracks of abrasive wear of the flank and rake surface were visible on microscope, which means that the cutting insert had good toughness and resistance to wear even when machining at higher cutting speeds. Increased feed results in increased flank wear. The smaller the feed, the less the wear, and as the feed increases, so does the wear. Increased feed results in increased amount of work of cutting insert. Increasing the feed affects the increase in cutting forces, and thus the increase in temperature. Increased feed results in increased chip thickness and accordingly increased cutting forces and temperature in the machining zone. In the present research the feed did not affect flank wear as much as corner radius and cutting speed, due to the ability of cutting insert to resist heat and fracture. Increased depth of cut can be of influence to the increase of dynamic loads, therefore to the increase of temperature. In the present research, the effect of depth of cut to the increase of flank wear is very small. The effect of depth of cut on flank wear is minimized by the hardness of CVD coating. Appropriate combination of feed and depth of cut can result in the mimimization of their common negative effect.

Flank wear appears as a result of abrasive wear. It is the result of friction between the cutting tool flank surface and the workpiece. The increased friction generates higher heat, i.e. temperature in the machining zone. In conditions of high temperatures, flank wear is intensified. The increase of cutting speed, feed and depth of cut results in the increase of friction between the turning insert and the workpiece. The increased friction generates higher temperature in the machining zone. The higher temperature, at the same value of the corner radius of turning insert, causes higher wear. At this, the cutting speed has a higher influence on temperature increase, feed has a smaller influence and depth of cut the smallest. By increasing corner radius of turning insert, the contact surface between the turning insert and the workpiece is increased while at smaller values of the turning insert radius the contact surface between the turning insert and the workpiece is reduced. For the same values of cutting speed, feed and depth of cut, if the contact surface is bigger (higher corner radius) the generated heat is disposed at the turning insert bigger surface so the turning insert wear is also smaller. Generally, at higher corner radii of turning inserts with smaller speed, feed and depth of cut, lower temperature is generated in the machining zone and at this, it is simultaneously disposed at the turning insert bigger surface. This directly causes reduction of the turning insert flank wear. At smaller corner radii of turning inserts, higher cutting speeds, feeds and depths of cut, higher temperature is generated in

Table 5 ANOVA table—flank wear *VB*

Source	Sum of squares	Degrees of freedom	Mean square	*F* value	*p* value Prob > *F*
Model	3.257144	11	0.296104	31,795.174	< 0.0001
A-Depth of cut	0.0184877	1	0.0184877	1985.176	< 0.0001
B-Feed	0.53918	1	0.53918	57,896.285	< 0.0001
C-Cutting speed	1.263252	1	1.263252	135,645.981	< 0.0001
D-Turning insert type	1.428868	3	0.476289171	51,143.170	< 0.0001
AB	8.99865×10^{-5}	1	8.99865×10^{-5}	9.66261	0.0023
BC	0.004918	1	0.004918	528.0912	< 0.0001
A^2	0.000136	1	0.000136	14.64466	0.0002
B^2	0.0001878	1	0.0001878	20.16897	< 0.0001
C^2	0.002025	1	0.002025	217.3922	< 0.0001
Residual	0.0012293	132	9.31286×10^{-6}		
R^2	0.99962		Standard deviation	0.0030517	
R^2 adjusted	0.999597		Mean	− 1.579915	
R^2 for prediction	0.999537		Coefficient of variation %	0.193156	
Adequate Precision	774.74377		Predicted residual sum of squares	0.001508	

Table 6 ANOVA table—surface roughness *Ra*

Source	Sum of squares	Degrees of freedom	Mean square	*F* value	*p* value Prob > *F*
Model	70.38974	15	4.692649315	36,865.844	< 0.0001
A-Depth of cut	0.1872923	1	0.1872923	1471.3839	< 0.0001
B-Feed	47.505607	1	47.505607	373,208.0125	< 0.0001
C-Cutting speed	0.0128186	1	0.0128186	100.70342	< 0.0001
D-Turning insert type	20.092089	3	6.697362817	52,615.0408	< 0.0001
AB	0.0203989	1	0.0203989	160.25527	< 0.0001
AD	0.0513925	3	0.017130835	134.58127	< 0.0001
BC	0.001527	1	0.001527	11.99699	0.0007
BD	2.3954387	3	0.798479556	6272.92198	< 0.0001
B^2	0.123176	1	0.123176	967.68074	< 0.0001
Residual	0.016293	128	0.00012729		
R^2	0.999769		Standard deviation	0.011282	
R^2 adjusted	0.9997414		Mean	1.666192	
R^2 for prediction	0.9996946		Coefficient of variation %	0.6771297	
Adequate Precision	734.0627022		Predicted residual sum of squares	0.021502375	

machining zone and is concentrated at the smaller contact surface of the turning insert. As a result, the wear of the turning insert is increased.

Duratomic CVD coating technique provides a balance between two opposite requirements—good hardness and good toughness of cutting insert. Besides, these cutting inserts are characterized by sharp cutting edges and zones enriched by cobalt and aluminium oxide. This helps to improve tribological effects at the point of contact of the workpiece and the cutting insert, i.e. there is less friction, which results in lower temperatures and contact pressures. In this way, mechanical properties of the cutting insert are improved as well as the thermal and chemical inertia in a wide range of possible input process parameters. Temperature reduction resulted in reduction of abrasive, adhesion and diffusion wear. Higher temperatures can reduce yield strength, therefore the workpiece hardness as well. High stresses and temperatures can cause flaking and chipping of material, thus causing formation of micro-welds on rake and flank surface of the cutting insert. Besides, specially

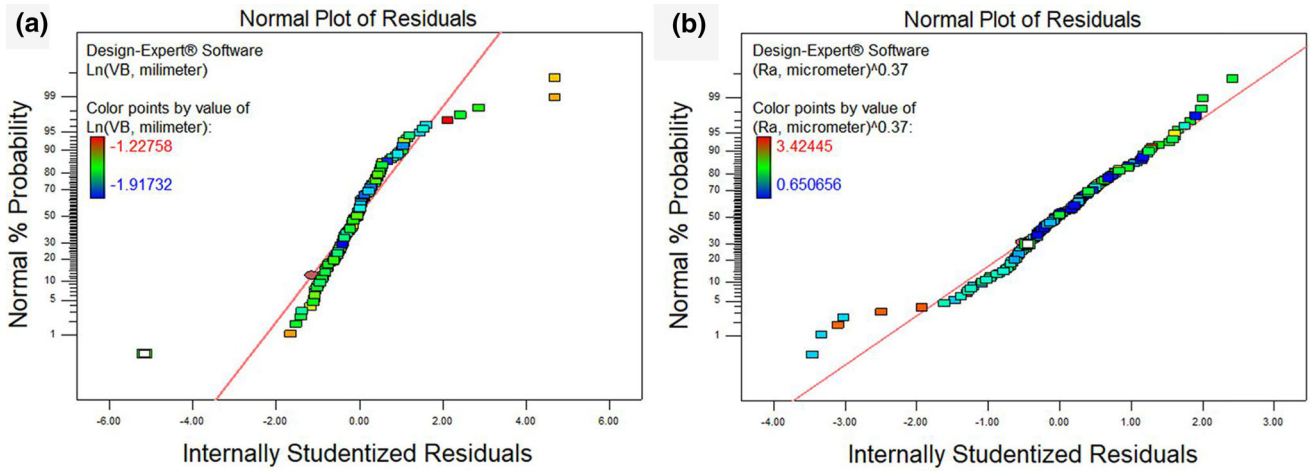

Fig. 2 Normal probability plot. **a** Flank wear *VB*, **b** surface roughness *Ra*

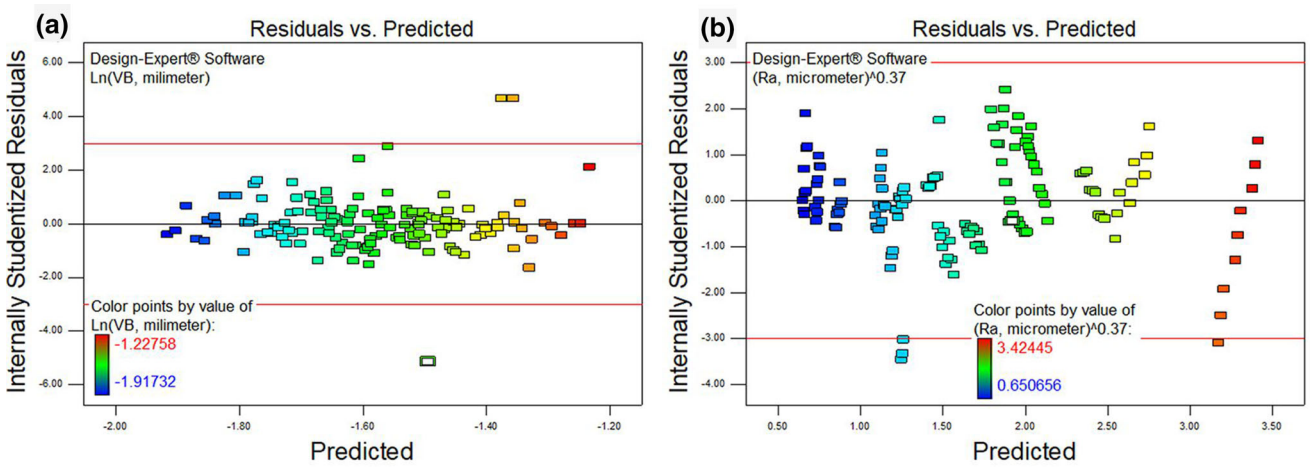

Fig. 3 Internally studentized residuals versus predicted values. **a** Flank wear *VB*, **b** surface roughness *Ra*

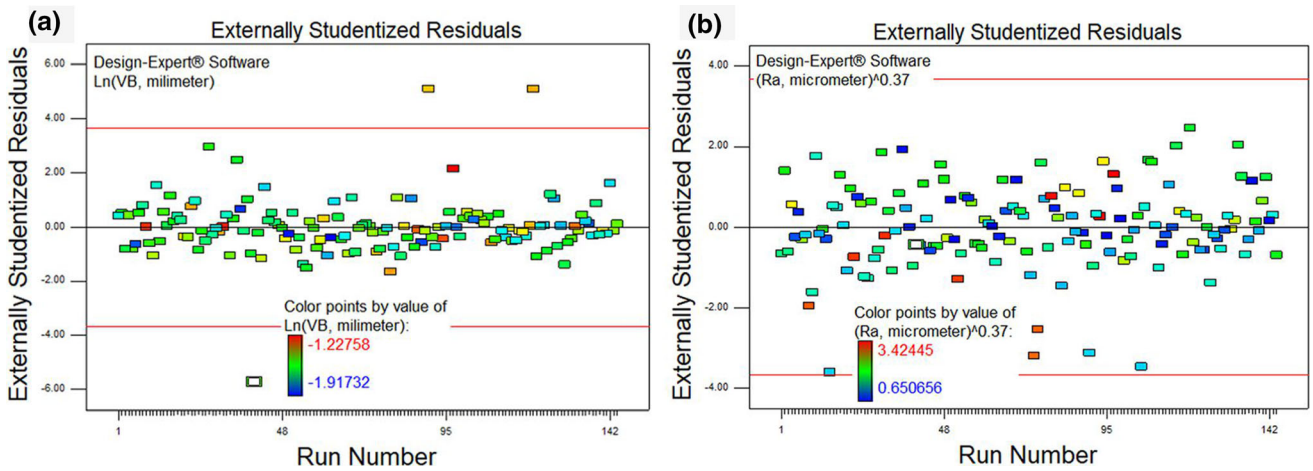

Fig. 4 Externally studentized residuals versus run number. **a** Flank wear *VB*, **b** surface roughness *Ra*

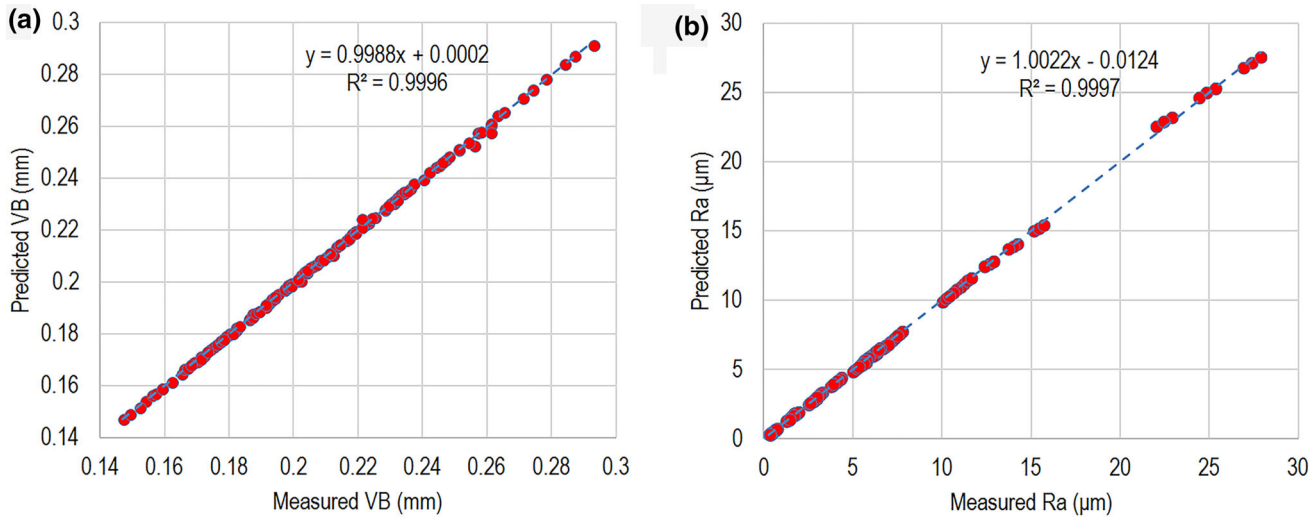

Fig. 5 Predicted versus measured values. **a** Flank wear *VB*, **b** surface roughness *Ra*

Table 7 Statistical measures for comparison of predicted and measured values

Response	Mean absolute error *MAE*	Root mean square error *RMSE*	Mean relative error *MRE*	Coefficient of correlation *R*
VB (mm)	0.000392	0.000639	0.00185	0.999779
Ra (μm)	0.06331	0.1075	0.0143	0.999856

designed geometry of chipbreaker is incorporated in the cutting insert which can be successfully used for the final as well as medium and rough machining. For selected levels of the input process parameters, this geometry provided reliable chip control and its breaking apart. During experimental researches, the chip short form was prevailing. This is the most desirable form of the chip considering the fact that it causes less damage.

The results of the regression analysis indicate that smaller surface roughness, i.e. better quality of machined surface, is achieved at smaller depths of cut, smaller feeds, smaller cutting speeds and higher radii of turning inserts (Fig. 7). Feed (correlation coefficient $r = 0.676$) and corner radius of turning insert ($r = -0.521$) exert the highest effect on surface roughness while the effect of depth of cut and cutting speed is small (correlation coefficients are $r = 0.058$ and $r = 0.014$).

There is interaction between feed and turning insert type (corner radius) (Fig. 8). At higher values of corner radius of turning insert (1.2 and 1.6 mm), by increasing feed, surface roughness increase is less expressed. At smaller corner radii of turning insert (0.8 mm) and particularly at the smallest corner radius of turning insert (0.4 mm) the effect of feed on surface roughness is more expressed, i.e. by higher feed, surface roughness increases fastest for the smallest corner radius of turning insert. At smaller feeds the effect of corner radius of turning insert on surface roughness is less expressed. At higher feeds the turning insert corner radius effect on surface roughness is more and more expressed and it increases as the feed increases. It can also be seen from Fig. 8 that higher corner radius of turning insert, at the same feed, generates smaller values of surface roughness i.e. better quality of machined surface. Higher values of feed at the same value of corner radius of turning insert generate higher values of surface roughness, i.e. worse quality of the machined surface. Increased surface roughness at small corner radii of turning inserts and higher feeds is the result of obtaining wider and higher peaks as well as of wider and higher valleys in the machined surface. Therefore, the highest surface roughness is achieved at the smallest corner radius of turning insert and the highest feed.

It was found that during the turning process, the surface roughness increases, in different amount, however, under different combinations of input parameters of machining. The surface roughness increase is similar to the trend of flank wear increase. It is more or less identical for all combinations of the input process parameters. These observations point to the strong interdependence of flank wear and surface roughness. It has to be pointed out that the technology of coating forming of used cutting inserts also provides for obtaining sharp cutting edges and smooth

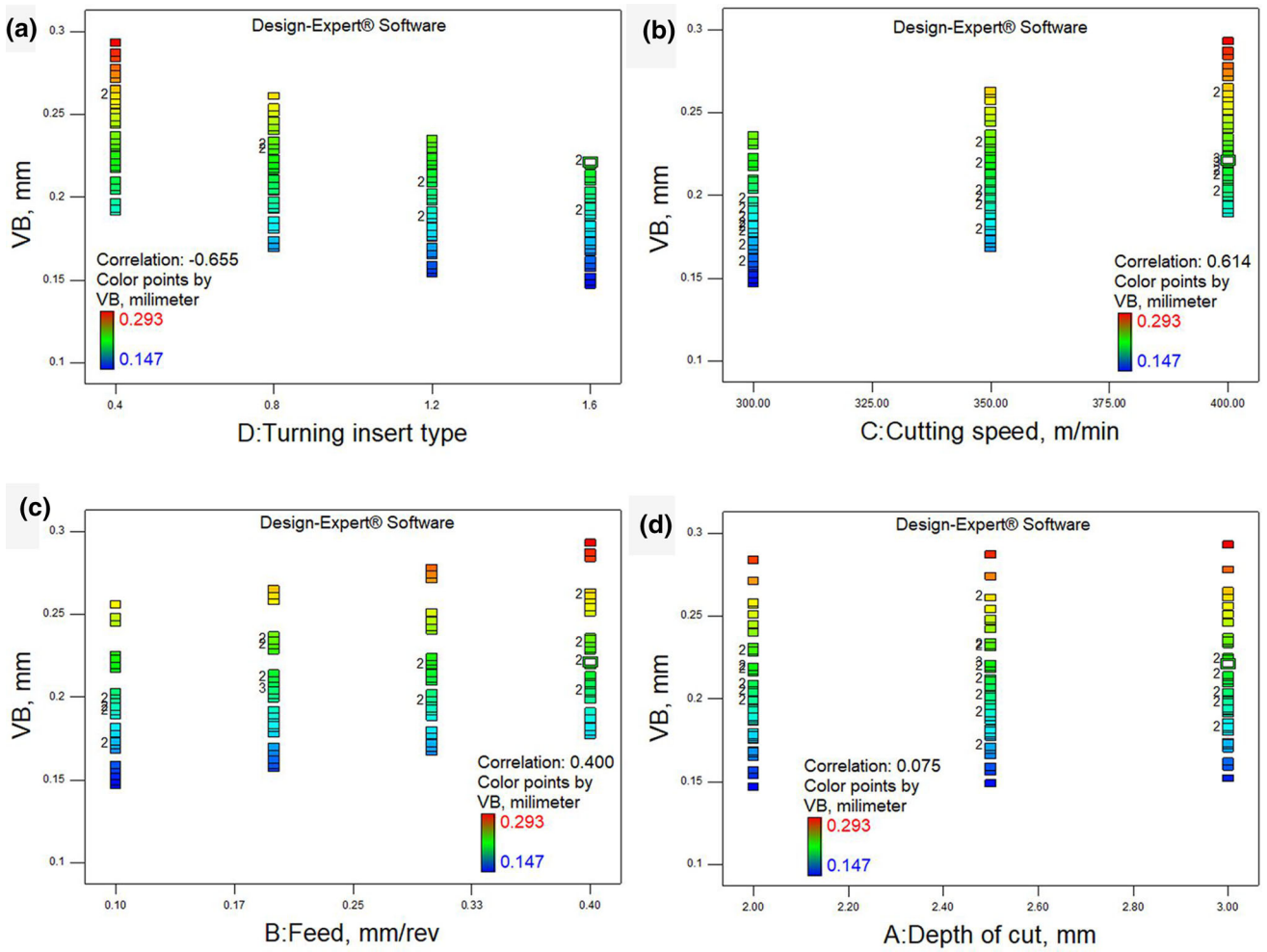

Fig. 6 Influence of machining parameters and corner radius of turning insert on flank wear. **a** Flank wear versus turning insert type, **b** flank wear versus cutting speed, **c** flank wear versus feed, **d** flank wear versus depth of cut

surface of a cutting insert which helps in obtaining smoother surface of the workpiece, and this again adds to creating more suitable tribological conditions i.e. smaller generation of friction and less generated heat in the zone of machining.

3.3 Multi-objective optimization

As introduced earlier, individual objective functions are minimization of flank wear (VB), minimization of surface roughness (Ra) and maximization of material removal rate (Q). Based on this, the following multi-objective function is defined:

$$F = \mathrm{MIN}(w_{VB} \cdot VB_x) + \mathrm{MIN}(w_{Ra} \cdot Ra_x) + \mathrm{MAX}(w_Q \cdot Q_x) \tag{19}$$

where w_{VB}, w_{Ra}, w_Q are weight coefficients, VB_x, Ra_x, Q_x are normalized—transformed values of output process parameters.

Normalized values of output process parameters are calculated using the following equations:

$$VB_x = \frac{VB - VB_{\min}}{VB_{\max} - VB_{\min}}, Ra_x = \frac{Ra - Ra_{\min}}{Ra_{\max} - Ra_{\min}}, Q_x = \frac{Q - Q_{\min}}{Q_{\max} - Q_{\min}} \tag{20}$$

It is however necessary to define the constraints, which limit the multi-objective optimization process to the desired feasible region. These constraints are defined by technological equipment performance (machine tool and measuring instrumentations), experimental research conditions and the obtained experimental results (Table 8).

After defining the objective function and boundary constraints for input parameters, the characteristic GA parameters must be set. When performing some initial test, it has been noticed that the objective function converges after approximately 200 iterations and stays within a narrow range for the rest of the optimization process, with the population size set to 100. In the current research, the

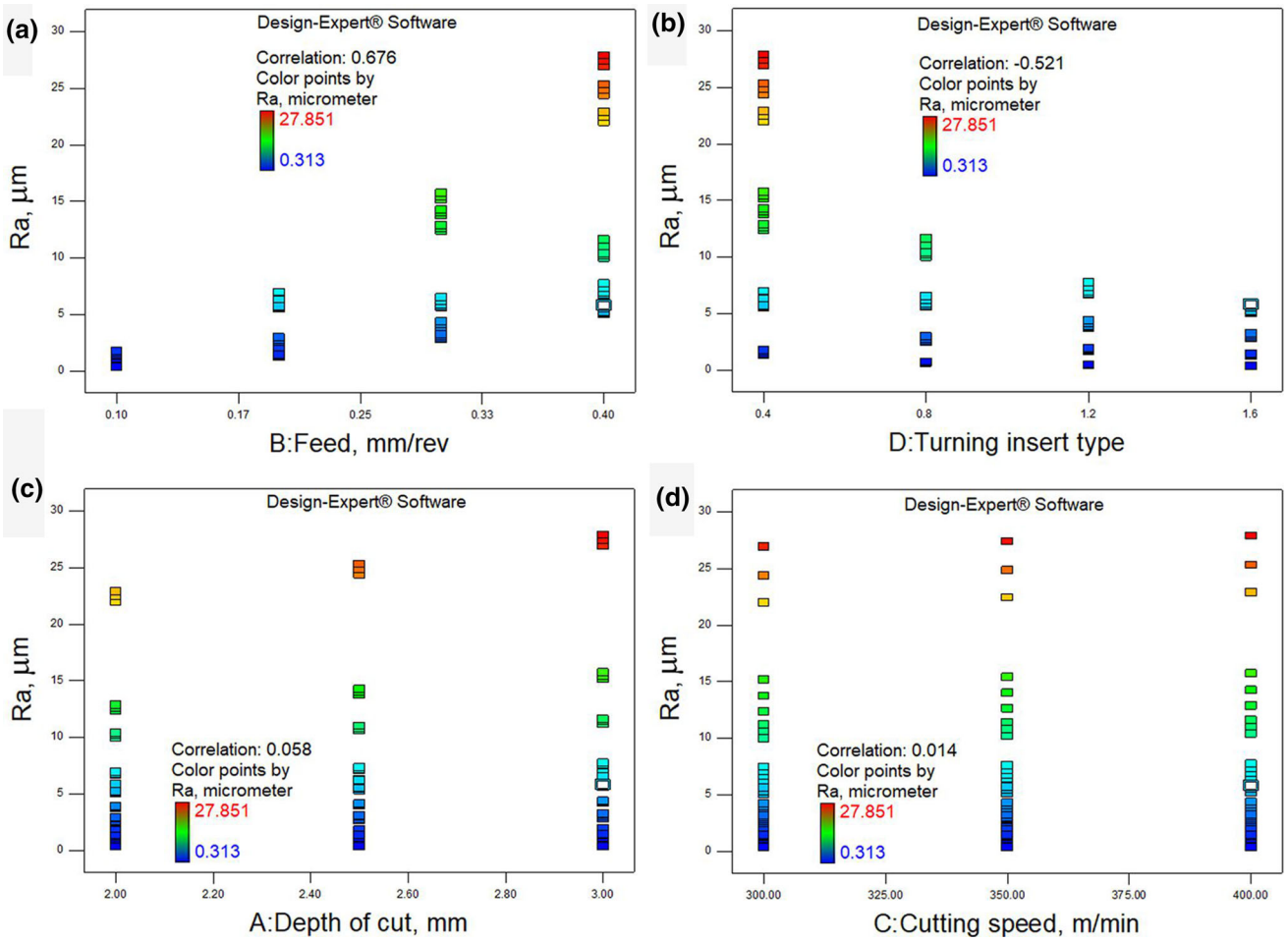

Fig. 7 Influence of machining parameters and corner radius of turning insert on surface roughness. **a** Surface roughness versus feed, **b** surface roughness versus turning insert type, **c** surface roughness versus depth of cut, **d** surface roughness versus cutting speed

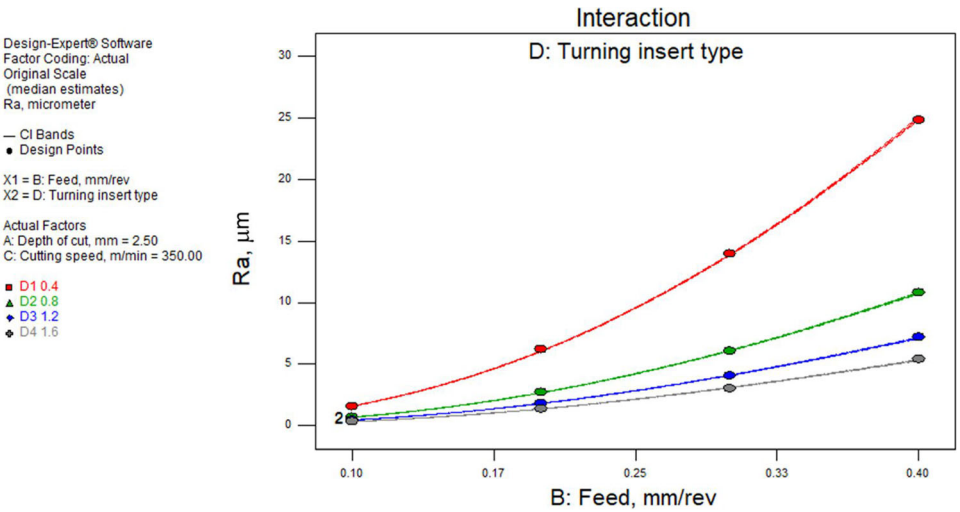

Fig. 8 Feed-turning insert type interaction

problem is solved offline, and the results are stored for the future use, so duration of the optimization process is not essential. Therefore, the maximum number of generations and the population size are set to 400 and 100, respectively, to ensure the quality of the optimization results. To the authors' best knowledge, the values of other GA parameters, crossover ratio, mutation rate, crossover fraction and Pareto front population fraction have more crucial

influence to the optimization quality. Setting of these parameters is a very complex task, since there is no exact recommendation for values of these parameters; it is strictly problem-dependent. Therefore, it is common to apply trial-and-error procedure to determine the appropriate parameter values. However, in this research, a more systematic approach has been applied. All parameter values have been varied in ranges recommended in the literature, listed in the previous chapter, and for each combination, the calculation of objective function value was performed. Based on the obtained results, the parameters providing the best value of the objective function have been chosen: crossover ratio is set to 1.2, mutation rate is set to 0.01, crossover fraction is set to 0.8 and Pareto front population fraction is set to 0.35. In order to determine the influence of GA parameter values to the optimization results and to confirm the parameter tuning procedure, a sensitivity analysis has been performed.

In order to conduct sensitivity analysis, the authors investigated how a change in GA parameters will affect a change in multi-objective function (expression 19). Four GA parameters, Pareto front fraction, crossover ratio, mutation rate and crossover fraction, were varied at three levels. The level adopted as optimal after the initial analysis was the reference, as shown in Table 9.

By statistical processing of all 81 (3^4) combinations of parameter levels, a significant quadratic reduced model was obtained with p value less than 0.05, which can be seen in Table 10 showing the analysis of variance. Some non-significant terms (A—Pareto front fraction, C—mutation rate and D—crossover fraction) are retained in the model because of the hierarchy. The terms which significantly contribute to the model are B—crossover ratio, interaction CD between mutation rate and crossover fraction as well as quadratic terms of all GA parameters.

Based on the response surface of the model, shown in Fig. 9, it was proved that the best value (minimum) of multi-objective function is achieved at the initially adopted level of GA parameters.

Thus, by the sensitivity analysis of GA parameters, it was proved that decreasing or increasing the value of the parameters relative to the optimal level would affect the increase of the multi-objective function value. It means that the initially adopted values (optimal ones) gave the best value (minimum) of multi-objective function.

Using the GA settings explained above, multi-objective optimization has been performed, resulting in optimal Pareto set consisting of totally 60 points. These points were used to generate the Pareto diagram shown in (Fig. 9) for the defined objective function (Eq. 19). The surface in the diagram (Fig. 9) represents an optimal surface, meaning that the points that are on the surface give one of the combinations of optimal solution, i.e. to every point of this surface corresponds one Pareto optimal solution of output process parameters—optimal surface roughness (Ra_{opt}), optimal flank wear (VB_{opt}) and optimal material removal rate (Q_{opt}). To every optimal combination of output process parameters corresponds an optimal combination of input process parameters—optimal feed (f_{opt}), optimal cutting speed (v_{copt}), optimal depth of cut (a_{popt}) and optimal corner radius (r_{opt}). It has to be mentioned that the surface shown in the diagram (Fig. 9) is obtained by cubic interpolation among 60 points which represent individual solutions obtained by genetic algorithm in a feasible region of possible optimal solutions (Fig. 10). The values of the output and input process parameters in the mentioned points are presented in Table 15 (Appendix).

Based on the results of multi-objective optimization, it can be concluded that the optimal surface roughness is in the range Ra_{opt} = 0.315–5.808 μm, optimal flank wear is in the range VB_{opt} = 0.150–0.218 mm, and optimal material removal rate is in the range Q_{opt} = 1088.384–8228.571 mm^3/s. Also, optimal value of corner radius of turning insert is always at maximal level r_{opt} = 1.6 mm. Optimal values of machining parameters cover the nearly complete feasible region i.e. ranges of input process parameters. Optimal value of feed is in the range f_{opt} = 0.10–0.40 mm/rev. Optimal value of cutting speed is in the range v_{copt} = 307–384 mm/min. Optimal value of depth of cut is in the range a_{popt} = 2.04–3 mm. In fact, it means that, for the given conditions of experimental research, turning has always to be performed with the turning insert of the highest corner radius, and that optimal combination of machining parameters can vary depending on production demands, i.e. on surface quality, tool life and productivity.

In order to substantially comprehend the influence of obtained results of multi-objective optimization, it is possible to divide the region of optimal solutions in Fig. 10 into 27 equal areas (Fig. 11, 2D displays, gray arrows). In this way, the individual, but also common influences of input process parameters on output process parameters can be easily observed. In accordance with this, a decomposition of each of the output process parameters is performed into three equal ranges (three levels)—low, mid and high. This is done by dividing the ranges of obtained optimal values (Ra_{opt} = 0.315–5.808 μm, VB_{opt} = 0.150–0.218 mm, Q_{opt} = 1088.384–8228.571 mm^3/s) into three equal parts (Table 11).

In an ideal case, for the three levels (three ranges in Table 11) and three variables (optimal levels of the output process parameters), all possible combinations, i.e. all together 3 × 3 × 3 = 27 combinations, can be generated. However, in this concrete case it is not possible to generate all the combinations in view of the fact that for some combinations (e.g. low Ra_{opt}, low VB_{opt}, high Q_{opt}; etc.) the areas do not exist in the region of feasible optimal values of

Table 8 Multi-objective optimization process constraints

Optimal parameter	Constraint	Value type	Decimal place	Description (constraint, value type, decimal place)
Feed f_{opt} (mm/rev)	$f_{min} \le f_{iopt} \le f_{max}$ $0.1 \le f_{iopt} \le 0.4$ $\forall i \in [1, \ldots, n]$	Continuous	3	In accordance with the experimental research conditions (recommendations of the manufacturer turning inserts), the accuracy of the machine tool and the possibility of setting the feed on the machine tool
Cutting speed v_{copt} (mm/min)	$v_{cmin} \le v_{ciopt} \le v_{cmax}$ $300 \le v_{ciopt} \le 400$ $\forall i \in [1, \ldots, n]$	Continuous	3	In accordance with the experimental research conditions (recommendations of the manufacturer turning inserts), the accuracy of the machine tool and the possibility of setting the cutting speed on the machine tool
Depth of cut a_{popt} (mm)	$a_{pmin} \le a_{piopt} \le a_{pmax}$ $2 \le a_{piopt} \le 3$ $\forall i \in [1, \ldots, n]$	Continuous	3	In accordance with the experimental research conditions (recommendations of the manufacturer turning inserts), the accuracy of the machine tool and the possibility of setting the depth of cut on the machine tool
Corner radius r_{iopt} (mm)	$r_{imin} \le r_{iopt} \le r_{imax}$ $r_{iopt} = 0.4 \vee 0.8 \vee 1.2 \vee 1.6$ $\forall i \in [1, \ldots, n]$	Categorical (discrete)	1	In accordance with the standard values of the corner radius of the manufacturer of turning inserts
Flank wear VB_{opt} (mm)	$VB_{min} \le VB_{iopt} \le VB_{max}$ $0.147 \le VB_{iopt} \le 0.293$ $\forall i \in [1, \ldots, n]$	Continuous	3	In accordance with the measuring range and accuracy of the measuring device used to measure flank wear
Surface roughness Ra_{opt} (μm)	$Ra_{min} \le Ra_{iopt} \le Ra_{max}$ $0.313 \le Ra_{iopt} \le 27.851$ $\forall i \in [1, \ldots, n]$	Continuous	3	In accordance with the measuring range and accuracy of the measuring device used to measure surface roughness
Material removal rate Q_{opt} (mm^3/s)	$Q_{min} \le Q_{iopt} \le Q_{max}$ $1041.67 \le Q_{iopt} \le 8571.43$ $\forall i \in [1, \ldots, n]$	Continuous	1	In accordance with the calculated experimental results

Table 9 The levels of GA parameters

	Minimum	Mean (optimum)	Maximum
Pareto front fraction	0.25	0.35	0.45
Crossover ratio	0.8	1.2	1.6
Mutation rate	0.005	0.01	0.015
Crossover fraction	0.7	0.8	0.9

output process parameters (Fig. 11). This is a consequence of the conflicting individual objective functions for *Ra*, *VB,* on the one hand and *Q,* on the other. In accordance with the foregoing, Table 12 displays possible combinations (for the regions for which solutions exist) of the optimal output process parameters along with the corresponding optimal combinations of the input process parameters.

The obtained results (Table 12) point to the following:

- high quality of machined surface (low level Ra_{opt}) can be realized in correspondence with small or medium flank wear (low level VB_{opt} and mid-level VB_{opt}) and small or mid-level productivity (low level Q_{opt} or mid-level Q_{opt}).
- mid-quality of machined surface (mid-level Ra_{opt}) can be realized only in correspondence with the simultaneous low flank wear and low productivity (low level VB_{opt} and low level Q_{opt}) or with the simultaneous mid-flank wear and mid-level productivities (mid-level VB_{opt} or mid-level Q_{opt}).
- high level of cutting tool life (low level VB_{opt}) can be realized only in correspondence with the simultaneous better quality of machined surface and low productivities (low level Ra_{opt} and low level Q_{opt}), or with better quality of machined surface and mid-level productivity (low level Ra_{opt} and mid-level Q_{opt}), or with mid-quality of machined surface and low level productivity (mid-level Ra_{opt} and low level Q_{opt}).
- mid-level of cutting tool life (mid-level VB_{opt}) can be realized in correspondence with the simultaneous low quality of machined surface and low productivity (low level Ra_{opt} and low level Q_{opt}), mid-quality of machined surface and mid-level of productivity (mid-level Ra_{opt} and mid-level Q_{opt}), low quality of machined surface and higher productivity (high Ra_{opt} and high Q_{opt}), as well as in combination of higher quality of machined surface and mid-level productivity (low level Ra_{opt} and mid-level Q_{opt}) and low quality of

Table 10 ANOVA table—multi-objective function

Source	Sum of squares	Degrees of freedom	Mean square	F value	p value Prob > F
Model	0.939997887	9	0.10444421	107.220069	< 0.0001
A-Pareto front fraction	0.000336002	1	0.000336002	0.34493173	0.5589
B-Crossover ratio	0.006225334	1	0.006225334	6.390787495	0.0137
C-Mutation rate	0.001348001	1	0.001348001	1.383827145	0.2434
D-Crossover fraction	0.002436135	1	0.002436135	2.500881223	0.1182
CD	0.00301401	1	0.00301401	3.094114659	0.0829
A^2	0.008267551	1	0.008267551	8.487281489	0.0048
B^2	0.18399526	1	0.18399526	188.8853826	< 0.0001
C^2	0.080249082	1	0.080249082	82.38189736	< 0.0001
D^2	0.654126511	1	0.654126511	671.511517	< 0.0001
Residual	0.069161855	71	0.000974111		
R^2	0.931465899		Standard deviation	0.031210746	
R^2 adjusted	0.922778478		Mean	0.937946914	
R^2 for prediction	0.911777907		Coefficient of variation %	3.327559916	
Adequate Precision	37.75476151		Predicted residual sum of squares	0.089030185	

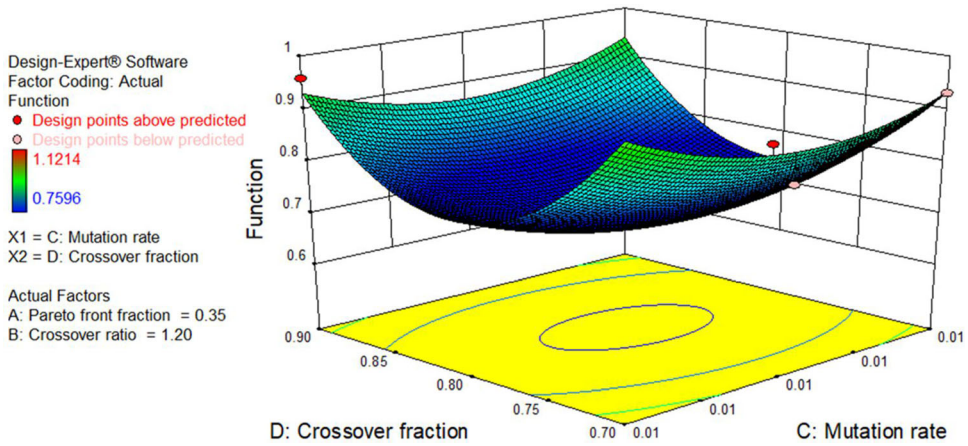

Fig. 9 3D response surface of multi-objective function

machined surface (high level Ra_{opt}) and mid-level productivity (mid-level Q_{opt}).

- mid-level productivity (mid-level Q_{opt}) can be realized in correspondence with the simultaneous higher quality of machined surface and/or low and mid-level flank wear (low level Ra_{opt} and/or low level VB_{opt}), mid-quality of machined surface and mid-level flank wear (mid-level Ra_{opt} and mid-level VB_{opt}), mid- or worse quality of machined surface and mid- or higher flank wear (mid- or high level Ra_{opt} and mid- and high level VB_{opt}).
- high productivity (high level Q_{opt}) can be realized in correspondence with mid- or low quality of machined surface (mid-level Ra_{opt} or high level Ra_{opt}) and/or mid- or low level of cutting tool life (mid-level VB_{opt} or high level VB_{opt}), but not with the simultaneous mid-quality of machined surface and mid-level of cutting tool life (mid-level Ra_{opt} and mid-level VB_{opt}).

For the purpose of validation of optimal points obtained by multi-objective optimization, confirmation experiments were conducted. The confirmation experiments were carried out in accordance with the plan presented in Table 13. The experiments were performed for 12 optimal points, i.e. 12 optimal combinations of input process parameters (f_{opt}, v_{copt}, a_{popt}, r_{opt}). Following the conducted additional experiments, measurement of flank wear (VB) and arithmetical mean roughness (Ra) was carried out. Ordinal numbers of optimal points shown in Table 13 correspond with ordinal numbers of optimal points presented in Figs. 10 and 11. Optimal combinations of input process parameters were selected to include the complete optimal surface shown in Figs. 10 and 11. This was done so that 10

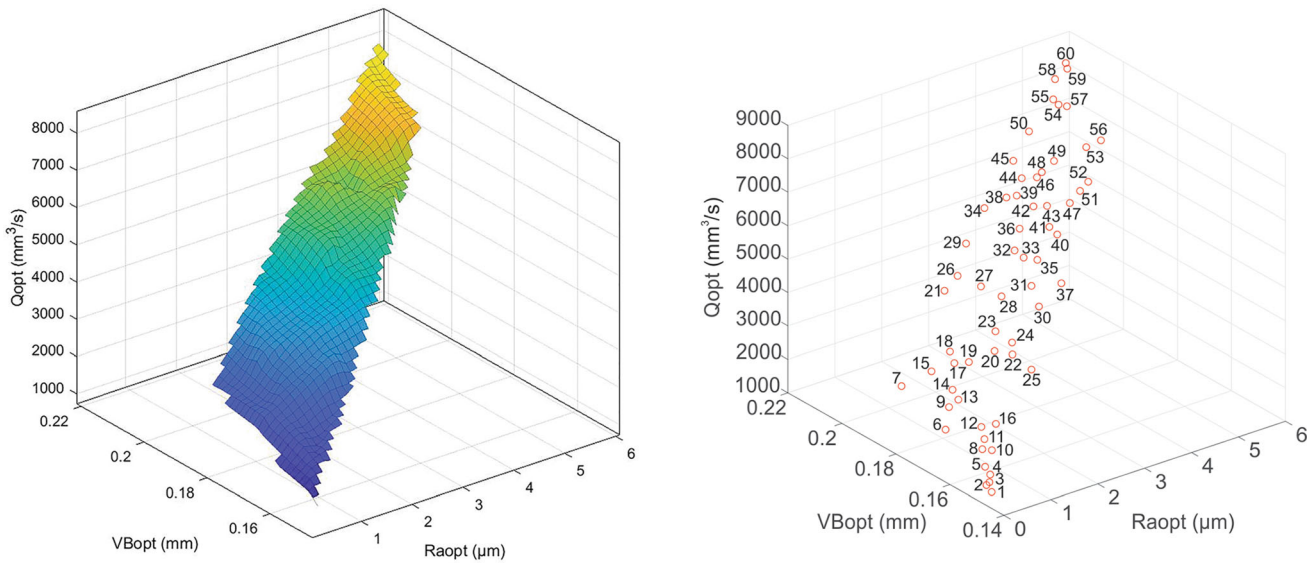

Fig. 10 Optimal surface and points for different combinations of output process parameters

optimal points were selected from the limits of optimal surface and 2 points from the mid-part of optimal surface. In this way, objectivity in the selection of points was achieved owing to the fact that all of the points were not concentrated in a single part of the optimal surface; this might have happened in the case of random selection of the points for confirmation.

Quantitative evaluation of obtained results was performed based on the following equations:

$$PE_{x_i} = \frac{\left|x_{ipov} - x_{imv}\right|}{x_{imv}} \cdot 100\% \quad i = 1, 2, \ldots, 12 \quad x = VB, Ra \tag{21}$$

$$MPE_x = \frac{100\%}{n} \sum_{i=1}^{n} \left| \frac{x_{ipov} - x_{imv}}{x_{imv}} \right| \quad i = 1, 2, \ldots, 12 \quad x = VB, Ra \tag{22}$$

where *PE*—percentage error, *MPE*—mean percentage error, x_{ipv}—predicted optimal value, x_{imv}—measured value.

Errors were calculated only for the output process parameters that were measured i.e. for flank wear (*VB*) and arithmetical mean roughness (*Ra*). Error was not calculated for material removal rate (*Q*), this being the output process parameter that was being calculated. Very low values of *PE* and *MPE* are to be noticed. *PE* for flank wear is in the range (1.130–1.878) %, for arithmetical mean roughness it is in the range (1.025–1.286) %. *MPE* are 1.478% and 1.146%, for flank wear and arithmetical mean roughness, respectively.

The same as for the regression models, the correlation between confirmed measured and obtained optimal GA values for *VB* and *Ra* is given in Fig. 12. The statistical measures—mean absolute error *MAE*, root mean square error *RMSE*, mean relative error *MRE* and coefficient of correlation *R* given in Table 14 prove that there is a very strong correlation between confirmed measured and obtained optimal GA values.

Finally, the calculated *p* values for the correlation between measured and obtained GA optimal values are much smaller than 0.05 which means that the correlation is statistically significant.

The results of multi-objective optimization support the hypothesis that it is possible to define a great number of optimal combinations of input parameters. At this the combination of optimal values of feed, cutting speed and depth of cut is interdependent. It depends on the requirements of output process parameters, i.e. on the importance and interrelation of surface quality, tool life and productivity.

With the increase of requirements for higher quality of machined surface, the importance of the machined surface roughness also increases. In these cases, if there are no high requirements for productivity, it is necessary to adopt feeds ranging from minimal level to somewhat less than mid-level (f_{opt} = 0.1–0.19 mm/rev), cutting speeds ranging from close to minimal level to close to mid-level (v_{copt} = 307–342 m/min) and depths of cut in a wide range from minimal to maximal level (a_{popt} = 2.04–2.9 mm). As the significance of productivity increases, feed also increases (f_{opt} = 0.23–0.25 mm/rev) as well as cutting speed (v_{copt} = 329–381 mm/rev) and depth of cut (a_{popt} = 2.53–2.82 mm). Higher corner radii of turning inserts ensure better quality of machined surface. In doing so, the higher radius compensates for the negative effect of increasing feed on the quality of machined surface. Therefore, the higher corner radius of turning insert enables

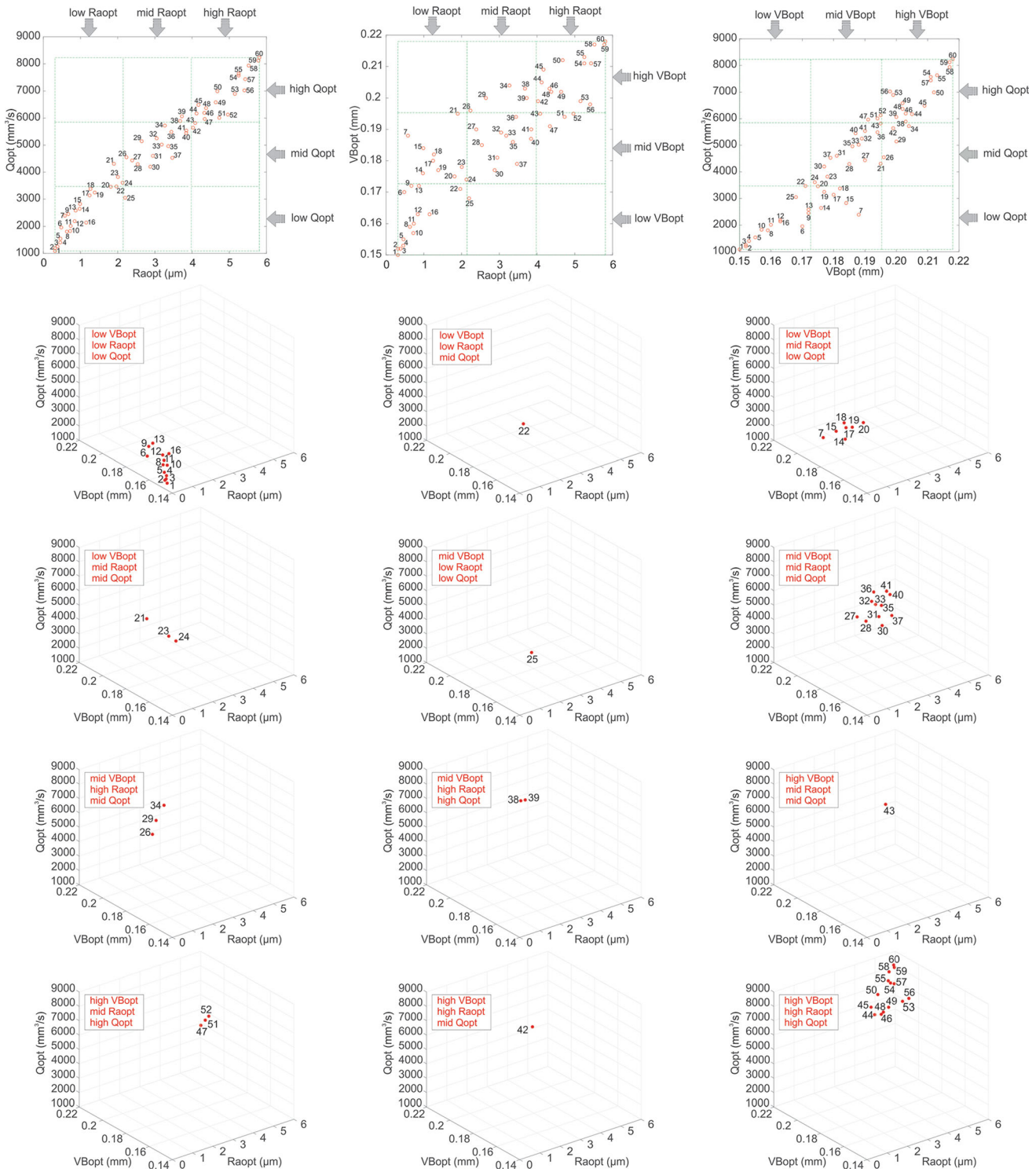

Fig. 11 Discretized areas—regions with optimal points in which there are combinations of output process parameters

the machining even with higher feeds and obtaining the corresponding quality of machined surface.

With increased requirements for dimensional accuracy and precision, higher requirements for geometric specifications of products and higher requirements for reducing costs, the importance of the turning insert wear also increases. In these cases, the feed should be adopted ranging from the minimal to the mid-level (f_{opt} = 0.1–0.24 mm/rev), depth of cut in a wide range from the minimal to the maximal level (a_{popt} = 2.04–2.9 mm), and

Table 11 Ranges of optimal output process parameters

Level	Output process parameters					
	Ra_{opt} (μm)		VB_{opt} (μm)		Q_{opt} (mm^3/s)	
	Range	Description	Range	Description	Range	Description
Low	0.315–2.131	High quality of machined surface	0.150–0.172	Low flank wear	1088.384–3456.706	Low productivity
Mid	2.199–3.846	Mid-quality of machined surface	0.174–0.195	Mid-flank wear	3468.370–5817.206	Mid-productivity
High	4.084–5.808	Low quality of machined surface	0.196–0.218	High flank wear	5892.356–8228.571	High productivity

Table 12 Possible combinations of optimal input and output process parameters

Case	Optimal point number (Figs. 5, 6, 7)	Output process parameters level			Optimal values of output process parameters			Optimal values of input process parameters			
		Ra_{opt}	VB_{opt}	Q_{opt}	Ra_{opt} (μm)	VB_{opt} (mm)	Q_{opt} (mm^3/s)	f_{opt} (mm/rev)	v_{copt} (m/min)	a_{popt} (mm)	r_{opt} (mm)
1	1, 2, 3, 4, 5, 6, 8, 9, 10, 11, 12, 13, 16	Low	Low	Low	0.315–1.153	0.15–0.172	1088.384–2586.276	0.1–0.19	307–342	2.04–2.9	1.6
2	22	Low	Low	Mid	1.966	0.171	3468.37	0.24	319	2.57	1.6
3	7, 14, 15, 17, 18, 19, 20	Low	Mid	Low	0.581–1.815	0.175–0.188	2394.66–3456.706	0.13–0.23	329–381	2.55–2.84	1.6
4	21, 23, 24	Low	Mid	Mid	1.899–2.131	0.174–0.195	3608.298–4307.589	0.23–0.25	324–374	2.53–2.82	1.6
5	25	Mid	Low	Low	2.199	0.168	3049.678	0.26	310	2.17	1.6
6	27, 28, 30, 31 32, 33, 35, 36, 37, 40, 41	Mid	Mid	Mid	2.389–3.846	0.177–0.194	4199.616–5537.449	0.26–0.33	319–357	2.52–2.96	1.6
7	26, 29, 34	Mid	High	Mid	2.236–3.268	0.196–0.204	4549.807–5722.441	0.25–0.3	372–378	2.76–2.85	1.6
8	38, 39	Mid	High	High	3.679–3.726	0.2–0.203	5892.356–6064.285	0.32	363–372	2.79–2.93	1.6
9	43	High	Mid	Mid	4.084	0.195	5817.206	0.34	347	2.78	1.6
10	47, 51, 52	High	Mid	High	4.34–4.962	0.191–0.195	5966.851–6129.646	0.35–0.38	334–340	2.69–2.87	1.6
11	42	High	High	Mid	4.025	0.199	5645.321	0.34	359	2.62	1.6
12	44, 45, 46, 48, 49, 50, 53, 54, 55, 56, 57, 58, 59, 60	High	High	High	4.121–5.808	0.198–0.218	6171.103–8228.571	0.34–0.4	340–384	2.73–3	1.6

cutting speed ranging from close to minimal level to close to mid-level (v_{copt} = 307–342 m/min). As the significance of productivity increases, feed also increases (f_{opt} = 0.23–0.25 mm/rev) as well as cutting speed (v_{copt} = 324–374 mm/rev) and depth of cut (a_{popt} = 2.53–2.82 mm). The level of the cutting speed, feed and depth of cut rises gently with the increase of requirements for higher productivity and decreases gently with the increase of requirements for the quality of machined surface.

By increasing the batch size and/or reducing the times of production, the importance of productivity also increases, i.e. the importance of material removal rate (chip quantity in time). In such cases, feeds should be adopted ranging from close to mid-level to maximal level (f_{opt} = 0.32–0.4 mm/rev), cutting speeds in the range from close to mid-level to close to maximal level (v_{copt} = 340–384 mm/rev) and depth of cut is either close to maximal level or is at the maximal level (a_{popt} = 2.69–3 mm). As the importance of the machined surface quality and the cutting insert wear increases, lower values of feed (close to the mid-level, f_{opt} = 0.32 mm/rev) and lower values of cutting speed (close to the mid-level v_{copt} = 334–340 mm/rev) should be adopted as well as higher values of the depth of cut (close to maximal level, a_{popt} = 2.79–2.87 mm). This is the result of the fact that

Table 13 Results of confirmation experiments

Optimal point	Optimal combinations of input process parameters				Calculated output process parameter	Predicted optimal output process parameters		Measured output process parameters		Percentage error	
	f_{opt} (mm/rev)	v_{copt} (mm/min)	a_{popt} (mm)	r_{opt} (mm)	Q_{opt} (mm^3/s)	VB_{opt} (mm)	Ra_{opt} (μm)	VB_{meas} (mm)	Ra_{meas} (μm)	PE_{VB} (%)	PE_{Ra} (%)
1	0.1	307	2.04	1.6	1088.384	0.150	0.315	0.152	0.311	1.316	1.286
6	0.12	342	2.7	1.6	1960.644	0.170	0.483	0.168	0.488	1.190	1.025
7	0.13	381	2.73	1.6	2394.66	0.188	0.581	0.185	0.574	1.622	1.220
16	0.19	316	2.05	1.6	2139.528	0.163	1.153	0.165	1.141	1.212	1.052
19	0.2	341	2.69	1.6	3245.163	0.177	1.383	0.174	1.367	1.724	1.170
25	0.26	310	2.17	1.6	3049.678	0.168	2.199	0.171	2.174	1.754	1.150
29	0.27	376	2.85	1.6	5142.556	0.200	2.646	0.197	2.674	1.523	1.047
37	0.32	319	2.52	1.6	4528.094	0.179	3.469	0.177	3.505	1.130	1.027
42	0.34	359	2.62	1.6	5645.321	0.199	4.025	0.202	3.974	1.485	1.283
45	0.34	381	2.82	1.6	6486.923	0.209	4.171	0.213	4.215	1.878	1.044
56	0.39	340	2.97	1.6	7025.867	0.198	5.406	0.195	5.339	1.538	1.255
60	0.4	384	3	1.6	8228.571	0.218	5.808	0.221	5.878	1.357	1.191
									Minimum *PE* (%)	1.130	1.025
									Maximum *PE* (%)	1.878	1.286
									MPE (%)	1.478	1.146

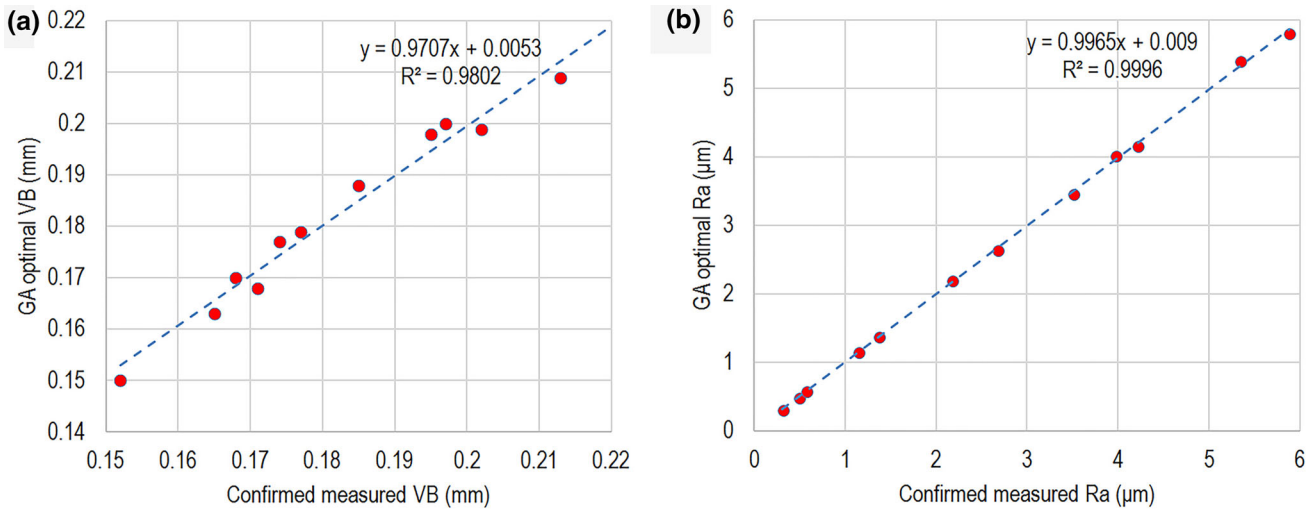

Fig. 12 Optimal GA versus measured values. **a** Flank wear *VB*, **b** surface roughness *Ra*

Table 14 Statistical measures for comparison of predicted GA optimal and measured values

Response	Mean absolute error *MAE*	Root mean square error *RMSE*	Mean relative error *MRE*	Coefficient of correlation *R*
VB (mm)	0.00275	0.00281	0.01478	0.990052
Ra (μm)	0.030417	0.03777	0.01146	0.999797

depth of cut has no essential impact on surface roughness and flank wear. In other words, the higher the importance of productivity for machining process, the higher depths of cut are to be used.

Based on the foregoing the following statements in connection with the common action of two of the three considered output process parameters can be presented. Better surface quality and higher tool life are achieved at smaller feeds and smaller cutting speeds. In case of smaller requirements for productivity, depth of cut is to be smaller. With increased requirements for productivity, it is desirable to increase depth of cut. The increased depth of cut has the least negative effect on surface roughness increase and flank wear. Better surface quality and higher productivity are achieved at smaller feed and higher depths of cut. In case of less requirements for tool wear, cutting speed is to be higher. With increasing requirements for smaller wear, it is desirable to keep cutting speed reducing. Increasing the depth of cut has the least negative effect on declining the surface quality and productivity. Longer tool life and higher productivity are achieved at smaller cutting speeds and higher depths of cut. In case of smaller requirements for surface quality, feed is to be higher. With increased requirements for better surface quality, it is desirable to reduce feed.

Lower levels of optimal combinations of values of surface roughness, flank wear and productivity (material removal rate) are achieved at maximal values of corner radius of turning insert (r_{opt} = 1.6 mm), feeds in the range from minimal values to those close to mid-level (f_{opt} = 0.1–0.19 mm/rev), cutting speeds in the range from minimal values to close to mid-values (v_{copt} = 307–342 m/min) and depths of cut in the wide range from minimal values to maximal values (a_{popt} = 2.04–2.9 mm). Productivity increase is easiest to achieve on account of depth of cut.

Mid-levels of optimal combinations of values of surface roughness, flank wear and productivity (material removal rate) are achieved at maximal values of corner radius of turning insert (r_{opt} = 1.6 mm), feeds that correspond to mid-values (f_{opt} = 0.26–0.233 mm/rev), cutting speeds in the range from those close to minimal value to those close to mid-value (v_{copt} = 319–357 m/min) and depths of cut in the range from mid-values to maximal values (a_{popt} = 2.52–2.96 mm). In this case, smaller values of cutting speed correspond to higher values of feed and vice versa.

Higher levels of optimal value combinations of surface roughness, flank wear and productivity (material removal rate) are achieved at maximal values of corner radius of turning insert (r_{opt} = 1.6 mm), feeds in the range from the values close to mid-values to maximal values (f_{opt} = 0.34–0.4 mm/rev), cutting speeds in the range from close to mid-values to close to maximal values (v_{copt} = 340–384 m/min) and depths of cut in the range from values close to mid-values to maximal values (a_{popt} = 2.73–3 mm).

Roughness of machined surface is a parameter of quality, which depends on geometric and technologic requirements of production. It may be an essential matter but a less essential as well in particular if some other finishing machining operation is performed after the operation of turning. As a rule, the flank wear of cutting insert directly affects the dimensional and geometric accuracy of machining. Apart from this it also affects machining costs considering the fact that the cutting insert which wears quicker becomes unusable and has to be replaced. The chip quantity is an essential output characteristic in case of larger batches or when production times are very short. In these cases, it is necessary to remove chip as soon as possible. That is why it is not always necessary to insist on general combination of optimal output process parameters. The essential point is to achieve the necessary values, i.e. optimal combinations in the complete feasible region. The achieved results of multi-objective optimization show that without regard to technological requirements of production, it is always suitable to perform turning with higher corner radii of turning inserts. This is the consequence of the fact that the turning inserts with bigger corner radius wear slower and at the same time generate a better quality surface i.e. surface with smaller roughness. Moreover, by increasing the importance of machined surface quality and/or tool life, machining should always be performed with higher corner radii of turning inserts, smaller cutting speeds, smaller feeds and higher depths of cut. With increased depth of cut, productivity (material removal rate) is also increased without notably affecting the surface quality and tool life.

4 Conclusion

In the present research, the authors conducted multi-objective optimization of cutting speed, feed, depth of cut and corner radius of turning insert from the point of their effect on the surface roughness, flank wear and material removal rate. Instead of the usual approach of obtaining only one combination of optimal parameters, a large number of combinations of optimal input process parameters were obtained, depending on the importance of each output process parameter, i.e. requirements of production.

Based on experimental researches, the arithmetical mean roughness of the surface is in the range Ra = 0.313–27.851 μm. This means that by an appropriate choice of the input process parameters exceptionally high quality of a machined surface can be obtained, but worse quality as well. In other words, by an appropriate

combination of the input process parameters the turning operation can be conducted as finish machining, medium machining and rough machining. Further on, a cutting insert flank wear covers the range of VB = 0.147–0.293 mm. The ratio maximum to minimum is approximately 2. This means that an appropriate combination of the input process parameters can result in a considerable influence on the intensity of cutting insert wear. Consequently, there is a possibility of considerable influence on the necessary dimensional accuracy and precision, geometric specifications and costs. To be noticed is also the possibility of considerable influence on productivity taking into consideration its wide range of Q = 1041.67–8571.43 mm^3/s.

Optimal combinations of input process parameters (Ra_{opt} = 0.315–5.808 μm, VB_{opt} = 0.150–0.218 mm, Q_{opt} = 1088.384–8228.571 mm^3/s) vary on a large scale. Optimal combinations of input process parameters depend on requirements defined in production plan, i.e. on importance of output process parameters. For different relations in importance of surface quality, tool life and productivity, different optimal combinations of input process parameters are obtained (Ra_{opt} = 0.315–5.808 μm, VB_{opt} = 0.150–0.218 mm, Q_{opt} = 1088.384–8228.571 mm^3/s). The trend of the optimal input parameters' influence on the optimal output process parameters is similar to that for experimental researches. It is of the essence to emphasize that there are very small differences in the ranges of experimental results and optimal results. This means that the possibilities will not be limited largely by optimization, and on the other hand, there is a possibility to have a considerable impact on obtaining better output parameters of the turning process.

The obtained results indicate that AISI 1040 steel workpiece turning with CVD coated turning inserts is convenient to perform with larger corner radii of turning inserts (r = 1.6 mm) regardless of production requirements. For the same machining parameters, turning inserts with larger corner radii always generate better quality of the machined surface and less flank wear, i.e. greater tool life. Depth of cut shows the least negative effect on flank wear and machined surface quality in terms of their getting worse. At the same time, higher depth of cut affects the increase of material removal rate. Therefore, optimal values of depth of cut increase with increase of the importance (weight) of productivity. It is appropriate to conduct machining with higher depths of cut for almost the complete feasible region of solutions. High depths of cut should not be applied only in case of small batches and in case the times of production are not short.

Earlier application of GA in turning operations indicated some disadvantages. Convergence of the GA is not always guaranteed. There exists no universal rule for selection of appropriate GA parameters. Also, GA may need substantial time to arrive at optimal solutions, accompanied by low speed of convergence and repeatability of results. Therefore, as a rule, a confirmation experiment is conducted to confirm or refute the validity of the model. The model is considered applicable in practice, if the MPE occurred is less than 5%, since these errors ensure that the turning operation is performed within the machining tolerances and the geometric product specifications. In this study, the results of confirmation experiments confirmed the validity of results obtained by optimization, proving that in spite of possible disadvantages, the solutions close to global optimum could be found by the use of genetic algorithm. The calculated PE and MPE, between the results obtained by multi-objective optimization and the results obtained by measuring after the confirmation experiments, are low. MPE of 1.478% for flank wear and 1.146% for arithmetical mean roughness are considered highly acceptable for practical application of multi-objective optimization based on genetic algorithm, in industry.

The applied methodology is limited to conditions, equipment and parameters used in performing this experimental research and to the workpiece material AISI 1040 steel. This presents its basic limitation. However, the methodology is quite generalized and universal so that with additional experimental researches it can also be applied to other machining operations, workpiece materials, conditions of machining, etc. In addition, all types of wear mechanisms and chip morphology will be analysed in detail in future research. Furthermore, future researches will be directed to considering higher number of input process parameters. This will contribute to the optimization of the process considering a higher number of criteria. In addition, in the future it is planned to develop, apply and compare the performance of different modeling and optimization techniques, as well as the development of hybrid approaches, in order to improve the turning process.

Appendix

See Table 15.

Table 15 Optimal combinations of input process parameters for different optimal combinations of output process parameters

Optimal point	Optimal combinations of output process parameters			Optimal combinations of input process parameters			
	Ra_{opt} (μm)	VB_{opt} (mm)	Q_{opt} (mm^3/s)	f_{opt} (mm/rev)	v_{copt} (mm/min)	a_{popt} (mm)	r_{opt} (mm)
1	0.315	0.150	1088.384	0.1	307	2.04	1.6
2	0.319	0.152	1201.549	0.1	310	2.22	1.6
3	0.382	0.152	1256.993	0.11	308	2.13	1.6
4	0.456	0.153	1405.273	0.12	308	2.18	1.6
5	0.463	0.155	1543.494	0.12	311	2.36	1.6
6	0.483	0.170	1960.644	0.12	342	2.7	1.6
7	0.581	0.188	2394.660	0.13	381	2.73	1.6
8	0.634	0.159	1807.467	0.14	315	2.34	1.6
9	0.672	0.172	2457.285	0.14	340	2.9	1.6
10	0.722	0.157	1828.125	0.15	310	2.25	1.6
11	0.736	0.160	2016.005	0.15	315	2.43	1.6
12	0.843	0.163	2194.135	0.16	320	2.44	1.6
13	0.871	0.172	2586.276	0.16	337	2.71	1.6
14	0.977	0.176	2650.096	0.17	347	2.55	1.6
15	0.989	0.184	2830.507	0.17	366	2.58	1.6
16	1.153	0.163	2139.528	0.19	316	2.05	1.6
17	1.246	0.180	3138.904	0.19	350	2.67	1.6
18	1.268	0.182	3374.928	0.19	352	2.84	1.6
19	1.383	0.177	3245.163	0.2	341	2.69	1.6
20	1.815	0.175	3456.706	0.23	329	2.59	1.6
21	1.899	0.195	4307.589	0.23	374	2.82	1.6
22	1.966	0.171	3468.370	0.24	319	2.57	1.6
23	2.007	0.178	3818.096	0.24	333	2.7	1.6
24	2.131	0.174	3608.298	0.25	324	2.53	1.6
25	2.199	0.168	3049.678	0.26	310	2.17	1.6
26	2.236	0.196	4549.807	0.25	372	2.76	1.6
27	2.389	0.190	4434.380	0.26	357	2.7	1.6
28	2.539	0.185	4295.735	0.27	344	2.62	1.6
29	2.646	0.200	5142.556	0.27	376	2.85	1.6
30	2.877	0.177	4199.616	0.29	321	2.56	1.6
31	2.947	0.181	4602.970	0.29	327	2.74	1.6
32	3.048	0.189	5251.061	0.29	343	2.96	1.6
33	3.183	0.188	5019.464	0.3	342	2.76	1.6
34	3.268	0.204	5722.441	0.3	378	2.84	1.6
35	3.360	0.186	4961.327	0.31	335	2.7	1.6
36	3.443	0.194	5490.819	0.31	351	2.84	1.6
37	3.469	0.179	4528.094	0.32	319	2.52	1.6
38	3.679	0.203	5892.356	0.32	372	2.79	1.6
39	3.726	0.200	6064.285	0.32	363	2.93	1.6
40	3.841	0.187	5448.819	0.33	331	2.81	1.6
41	3.846	0.190	5537.449	0.33	339	2.79	1.6
42	4.025	0.199	5645.321	0.34	359	2.62	1.6
43	4.084	0.195	5817.206	0.34	347	2.78	1.6
44	4.121	0.205	6171.103	0.34	371	2.76	1.6
45	4.171	0.209	6486.923	0.34	381	2.82	1.6
46	4.329	0.203	6193.335	0.35	366	2.73	1.6
47	4.340	0.191	5966.851	0.35	334	2.87	1.6

Table 15 (continued)

Optimal point	Optimal combinations of output process parameters			Optimal combinations of input process parameters			
	Ra_{opt} (μm)	VB_{opt} (mm)	Q_{opt} (mm^3/s)	f_{opt} (mm/rev)	v_{copt} (mm/min)	a_{popt} (mm)	r_{opt} (mm)
48	4.376	0.202	6369.139	0.35	362	2.83	1.6
49	4.636	0.202	6584.845	0.36	357	2.88	1.6
50	4.679	0.212	6992.740	0.36	382	2.86	1.6
51	4.730	0.194	6009.966	0.37	340	2.7	1.6
52	4.962	0.195	6129.646	0.38	339	2.69	1.6
53	5.150	0.199	6895.276	0.38	345	2.95	1.6
54	5.251	0.211	7572.857	0.38	372	3	1.6
55	5.252	0.213	7638.861	0.38	378	2.98	1.6
56	5.406	0.198	7025.867	0.39	340	2.97	1.6
57	5.429	0.211	7441.366	0.39	371	2.89	1.6
58	5.521	0.217	7935.096	0.39	384	2.97	1.6
59	5.782	0.217	8117.366	0.4	383	2.97	1.6
60	5.808	0.218	8228.571	0.4	384	3	1.6

Acknowledgements The results presented in this paper are obtained in the framework of the Project No. SV001 entitled "Modelling and optimizing processes applicable in maintenance" funded by the University of Slavonski Brod, Mechanical Engineering Faculty in Slavonski Brod, Republic of Croatia, and within the Project No. 451-03-68/2020-14/200156 entitled "Innovative scientific and artistic research from the FTS (activity) domain" funded by the Ministry of Education, Science and Technological Development of Republic of Serbia.

Declarations

Conflict of interest The authors declare that they have no conflict of interest.

References

1. Gok A (2015) A new approach to minimization of the surface roughness and cutting force via fuzzy TOPSIS, multi-objective grey design and RSA. Measurement 70:100–109. https://doi.org/10.1016/j.measurement.2015.03.037
2. Dureja J, Gupta V, Sharma VS, Dogra M, Bhatti MS (2016) A review of empirical modeling techniques to optimize machining parameters for hard turning applications. Proc Inst Mech Eng B J Eng Manuf 230:389–404. https://doi.org/10.1177/0954405414558731
3. Singh R, Dureja JS, Dogra M, Randhawa JS (2019) Optimization of machining parameters under MQL turning of Ti–6Al–4V alloy with textured tool using multi-attribute decision-making methods. World J Eng 16:648–659. https://doi.org/10.1108/WJE-06-2019-0170
4. Nguyen TT (2020) An energy-efficient optimization of the hard turning using rotary tool. Neural Comput Appl. https://doi.org/10.1007/s00521-020-05149-2
5. Tuffy K, Byrne G, Dowling D (2004) Determination of the optimum TiN coating thickness on WC inserts for machining carbon steels. J Mater Process Technol 155–156:1861–1866. https://doi.org/10.1016/j.jmatprotec.2004.04.277
6. Gunay M, Seker U, Sur G (2006) Design and construction of a dynamometer to evaluate the influence of cutting tool rake angle on cutting forces. Mater Des 27:1097–1101. https://doi.org/10.1016/j.matdes.2005.04.003
7. Yaldiz S, Unsacar F, Saglam H (2006) Comparison of experimental results obtained by designed dynamometer to fuzzy model for predicting cutting forces in turning. Mater Des 27(10):1139–1147. https://doi.org/10.1016/j.matdes.2005.03.010
8. Saglam H, Unsacar F, Yaldiz S (2006) Investigation of the effect of rake angle and approaching angle on main cutting force and tool tip temperature. Int J Mach Tools Manuf 46:132–141. https://doi.org/10.1016/j.ijmachtools.2005.05.002
9. Salgado DR, Alonso FJ (2007) An approach based on current and sound signals for in-process tool wear monitoring. Int J Mach Tools Manuf 47:2140–2152. https://doi.org/10.1016/j.ijmachtools.2007.04.013
10. Asilturk I, Cunkas M (2011) Modeling and prediction of surface roughness in turning operations using artificial neural network and multiple regression method. Expert Syst Appl 38:5826–5832. https://doi.org/10.1016/j.eswa.2010.11.041
11. Neseli S, Yaldiz S, Turkes E (2011) Optimization of tool geometry parameters for turning operations based on the response surface methodology. Measurement 44(3):580–587. https://doi.org/10.1016/j.measurement.2010.11.018
12. Topal ES, Cogun C (2011) Computer-based estimation and compensation of diametral errors in CNC turning of cantilever bars. J Intell Manuf 22:853–865. https://doi.org/10.1007/s10845-009-0360-0
13. Cohen G, Gilles P, Segonds S, Mousseigne M, Lagarrigue P (2012) Thermal and mechanical modeling during dry turning operations. Int J Adv Manuf Technol 58:133–140. https://doi.org/10.1007/s00170-011-3372-9
14. Asilturk I (2012) Predicting surface roughness of hardened AISI 1040 based on cutting parameters using neural networks and multiple regression. Int J Adv Manuf Technol 63:249–257. https://doi.org/10.1007/s00170-012-3903-z
15. Venkata Rao K, Murthy BSN, Mohan Rao N (2013) Cutting tool condition monitoring by analyzing surface roughness, work piece vibration and volume of metal removed for AISI 1040 steel in boring. Measurement 46:4075–4084. https://doi.org/10.1016/j.measurement.2013.07.021

16. Venkata Rao K, Murthy B, Mohan Rao N (2015) Experimental study on surface roughness and vibration of workpiece in boring of AISI 1040 steels. Proc Inst Mech Eng B J Eng Manuf 229:703–712. https://doi.org/10.1177/0954405414531247
17. Prasad BS, Babu MP, Reddy YR (2016) Evaluation of correlation between vibration signal features and three-dimensional finite element simulations to predict cutting tool wear in turning operation. Proc Inst Mech Eng B J Eng Manuf 230:203–214. https://doi.org/10.1177/0954405414554018
18. Venkata Rao K, Vidhu KP, Kumar TA, Rao NN, Murthy PBGSN, Balaji M (2016) An artificial neural network approach to investigate surface roughness and vibration of workpiece in boring of AISI1040 steels. Int J Adv Manuf Technol 83:919–927. https://doi.org/10.1007/s00170-015-7621-1
19. Yadav RN (2017) A hybrid approach of Taguchi-response surface methodology for modeling and optimization of duplex turning process. Measurement 100:131–138. https://doi.org/10.1016/j.measurement.2016.12.060
20. Haque T, Kumar S, Upadhaya D, Barman M, Mukhopadhyay A (2017) Optimization of multiple roughness characteristics for turning of AISI 1040 steel under different cutting conditions. Int J Eng Technol 10:1–10. https://doi.org/10.18052/www.scipress.com/ijet.10.1
21. Akkus H (2018) Optimising the effect of cutting parameters on the average surface roughness in a turning process with the Taguchi method. Mater Tehnol 52:781–785. https://doi.org/10.17222/mit.2018.110
22. Jhodkar D, Amarnath M, Chelladurai H, Ramkumar J (2018) Performance assessment of microwave treated WC insert while turning AISI 1040 steel. J Mech Sci Technol 32:2551–2558. https://doi.org/10.1007/s12206-018-0512-2
23. Jhodkar D, Amarnath M, Chelladurai H, Ramkumar J (2018) Experimental investigations to enhance the machining performance of tungsten carbide tool insert using microwave treatment process. J Braz Soc Mech Sci Eng. https://doi.org/10.1007/s40430-018-1096-6
24. Dhar NR, Paul S, Chattopadhyay AB (2002) The influence of cryogenic cooling on tool wear, dimensional accuracy and surface finish in turning AISI 1040 and E4340C steels. Wear 249:932–942. https://doi.org/10.1016/s0043-1648(01)00825-0
25. Dhar NR, Ahmed MT, Islam S (2007) An experimental investigation on effect of minimum quantity lubrication in machining AISI 1040 steel. Int J Mach Tools Manuf 47:748–753. https://doi.org/10.1016/j.ijmachtools.2006.09.017
26. Vamsi Krishna P, Rao DN, Srikant RR (2009) Predictive modelling of surface roughness and tool wear in solid lubricant assisted turning of AISI 1040 steel. Proc Inst Mech Eng J Eng Tribol 223:929–934. https://doi.org/10.1243/13506501jet475
27. Ramana SV, Ramji K, Satyanarayana B (2010) Studies on the behaviour of the green particulate fluid lubricant in its nano regime when machining AISI 1040 steel. Proc Inst Mech Eng B J Eng Manuf 224:1491–1501. https://doi.org/10.1243/09544054jem1862
28. Vamsi Krishna P, Srikant RR, Nageswara Rao D (2010) Experimental investigation on the performance of nanoboric acid suspensions in SAE-40 and coconut oil during turning of AISI 1040 steel. Int J Mach Tools Manuf 50:911–916. https://doi.org/10.1016/j.ijmachtools.2010.06.001
29. Amrita M, Srikant R, Sitaramaraju A, Prasad M, Krishna PV (2013) Experimental investigations on influence of mist cooling using nanofluids on machining parameters in turning AISI 1040 steel. Proc Inst Mech Eng J Eng Tribol 227:1334–1346. https://doi.org/10.1177/1350650113491934
30. Srikiran S, Ramji K, Satyanarayana B, Ramana S (2014) Investigation on turning of AISI 1040 steel with the application of nano-crystalline graphite powder as lubricant. Proc Inst Mech Eng C J Mech Eng Sci 228:1570–1580. https://doi.org/10.1177/0954406213509612
31. Gupta MK, Singh G, Sood PK (2015) Experimental investigation of machining AISI 1040 medium carbon steel under cryogenic machining: a comparison with dry machining. J Inst Eng India Ser C 96:373–379. https://doi.org/10.1007/s40032-015-0178-9
32. Padmini R, Krishna PV, Mohana Rao GK (2016) Experimental evaluation of nano-molybdenum disulphide and nano-boric acid suspensions in vegetable oils as prospective cutting fluids during turning of AISI 1040 steel. Proc Inst Mech Eng J Eng Tribol 230:493–505. https://doi.org/10.1177/1350650115601694
33. Ajay Vardhaman BS, Amarnath M, Jhodkar D, Ramkumar J, Chelladurai H, Roy MK (2018) Influence of coconut oil on tribological behavior of carbide cutting tool insert during turning operation. J Braz Soc Mech Sci Eng. https://doi.org/10.1007/s40430-018-1379-y
34. Mia M, Dhar NR (2019) Prediction and optimization by using SVR, RSM and GA in hard turning of tempered AISI 1060 steel under effective cooling condition. Neural Comput Appl 31:2349–2370. https://doi.org/10.1007/s00521-017-3192-4
35. Usha M, Rao GS (2020) Optimization of multiple objectives by genetic algorithm for turning of AISI 1040 steel using Al_2O_3 nano fluid with MQL. Trib Ind 42:70–80. https://doi.org/10.24874/ti.2020.42.01.07
36. Sahinoglu A, Rafighi M (2020) Optimization of cutting parameters with respect to roughness for machining of hardened AISI 1040 steel. Mater Test 62:85–95. https://doi.org/10.3139/120.111458
37. Gugulothu S, Pasa VK (2020) Experimental investigation to study the performance of CNT/MoS_2 hybrid nanofluid in turning of AISI 1040 steel. Aust J Mech Eng. https://doi.org/10.1080/14484846.2020.1756067
38. Yildiz AR (2012) A comparative study of population-based optimization algorithms for turning operations. Inf Sci 210:81–88. https://doi.org/10.1016/j.ins.2012.03.005
39. Ahilan C, Kumanan S, Sivakumaran N, Edwin Raja Dhas J (2013) Modeling and prediction of machining quality in CNC turning process using intelligent hybrid decision making tools. Appl Soft Comput 13:1543–1551. https://doi.org/10.1016/j.asoc.2012.03.071
40. Chandrasekaran M, Muralidhar M, Krishna CM, Dixit US (2010) Application of soft computing techniques in machining performance prediction and optimization: a literature review. Int J Adv Manuf Technol 46:445–464. https://doi.org/10.1007/s00170-009-2104-x
41. Garg A, Bhalerao Y, Tai K (2013) Review of empirical modelling techniques for modelling of turning process. Int J Model Identif Control 20:121–129. https://doi.org/10.1504/ijmic.2013.056184
42. Sibalija TV (2019) Particle swarm optimisation in designing parameters of manufacturing processes: A review (2008–2018). Appl Soft Comput 84:105743. https://doi.org/10.1016/j.asoc.2019.105743
43. Yusup N, Zain AM, Hashim SZM (2012) Evolutionary techniques in optimizing machining parameters: review and recent applications (2007–2011). Expert Syst Appl 39:9909–9927. https://doi.org/10.1016/j.eswa.2012.02.109
44. Leo Kumar SP (2017) State of the art-intense review on artificial intelligence systems application process i planning and manufacturing. Eng Appl Artif Intell 65:294–329. https://doi.org/10.1016/j.engappai.2017.08.005
45. Sterpin Valic G, Cukor G, Jurkovic Z, Brezocnik M (2019) Multi-criteria optimization of turning of martensitic stainless steel for sustainability. Int J Simul Model 18:632–642. https://doi.org/10.2507/IJSIMM18(4)495

46. Ghosh T, Martinsen K (2020) Generalized approach for multi-response machining process optimization using machine learning and evolutionary algorithms. Eng Sci Technol Int J 23:650–663. https://doi.org/10.1016/j.jestch.2019.09.003
47. Chavez-Garcia H, Castillo-Villar KK (2018) Simulation-based model for the optimization of machining parameters in a metal-cutting operation. Simul Model Pract Theory 84:204–221. https://doi.org/10.1016/j.simpat.2018.02.008
48. Weichert D, Link P, Stoll A, Ruping S, Ihlenfeldt S, Wrobel S (2019) A review of machine learning for the optimization of production processes. Int J Adv Manuf Technol 104:1889–1902. https://doi.org/10.1007/s00170-019-03988-5
49. Rana N, Latiff MSA, Abdulhamid SM, Chiroma H (2020) Whale optimization algorithm: a systematic review of contemporary applications, modifications and developments. Neural Comput Appl 32:16245–16277. https://doi.org/10.1007/s00521-020-04849-z
50. Srinivasan S, Ramakrishnan S (2011) Evolutionary multi objective optimization for rule mining: a review. Artif Intell Rev 36:205–248. https://doi.org/10.1007/s10462-011-9212-3
51. Ojha M, Singh KP, Chakraborty P, Verma S (2019) A review of multi-objective optimisation and decision making using evolutionary algorithms. Int J Bio Inspir Com 14:69. https://doi.org/10.1504/ijbic.2019.101640
52. Liu Q, Li X, Liu H, Guo Z (2020) Multi-objective metaheuristics for discrete optimization problems: a review of the state-of-the-art. Appl Soft Comput 93:106382. https://doi.org/10.1016/j.asoc.2020.106382
53. Gullu H (2017) A novel approach to prediction of rheological characteristics of jet grout cement mixtures via genetic expression programming. Neural Comput Appl 28:407–420. https://doi.org/10.1007/s00521-016-2360-2
54. Quiza Sardinas R, Rivas Santana M, Alfonso Brindis E (2006) Genetic algorithm-based multi-objective optimization of cutting parameters in turning processes. Eng Appl Artif Intell 19:127–133. https://doi.org/10.1016/j.engappai.2005.06.007
55. D'Addona DM, Teti R (2013) Genetic algorithm-based optimization of cutting parameters in turning processes. Procedia CIRP 7:323–328. https://doi.org/10.1016/j.procir.2013.05.055
56. Lv J, Zhao JB, Liu QG (2013) Optimization of cutting parameters based on multi-objective genetic algorithm NSGA- II. Appl Mech Mater 281:517–522. https://doi.org/10.4028/www.scientific.net/amm.281.517
57. Klancnik S, Hrelja M, Balic J, Brezocnik M (2016) Multi-objective optimization of the turning process using a gravitational search algorithm (GSA) and NSGA-II approach. Adv Prod Eng Manag 11:366–376. https://doi.org/10.14743/apem2016.4.234
58. Manav O, Chinchanikar S (2018) Multi-objective optimization of hard turning: a genetic algorithm approach. Mater Today 5:12240–12248. https://doi.org/10.1016/j.matpr.2018.02.201
59. Sathiya Narayanan N, Baskar N, Ganesan M (2018) Multi objective optimization of machining parameters for hard turning OHNS/AISI H13 material, using genetic algorithm. Mater Today 5:6897–6905. https://doi.org/10.1016/j.matpr.2017.11.351
60. Venkatesan D, Kannan K, Saravanan R (2009) A genetic algorithm-based artificial neural network model for the optimization of machining processes. Neural Comput Appl 18:135–140. https://doi.org/10.1007/s00521-007-0166-y
61. Jasiewicz M, Miadlicki K (2020) An integrated CNC system for chatter suppression in turning. Adv Prod Eng Manag 15:318–330. https://doi.org/10.14743/apem2020.3.368
62. Yang MS, Ba L, Xu EB, Li Y, Gao XQ, Liu Y, Li Y (2019) Batch optimization in integrated scheduling of machining and assembly. Int J Simul Model 18:689–698. https://doi.org/10.2507/IJSIMM18(4)CO17
63. Tschatsch H (2009) Applied machining technology. Springer, Berlin. https://doi.org/10.1007/978-3-642-01007-1
64. Kalyanmoy D (2001) Multi-objective optimization using evolutionary algorithms. Wiley, Chichester

Publisher's Note Springer Nature remains neutral with regard to jurisdictional claims in published maps and institutional affiliations.